NASA
Technical
Memorandum

NASA TM- 108472

VEHICLE HEALTH MANAGEMENT USING ADAPTIVE TECHNIQUES—CDDF FINAL REPORT (No. 92-12)

By J.H. Kim and R. Kissel

Program Development Office

November 1994

NASA
National Aeronautics and
Space Administration

George C. Marshall Space Flight Center

TABLE OF CONTENTS

LIST OF ILLUSTRATIONS

LIST OF ILLUSTRATIONS (Continued)

LIST OF TABLES

ABBREVIATIONS AND ACRONYMS

ABS	absolute value
ANN	artificial neural network
CDDF	Center Director's Discretionary Fund
DFT	discrete Fourier transform
DSP	digital signal processor
HPOTP	high pressure oxygen turbopump
Hz	Hertz
MSFC	Marshall Space Flight Center
SF	synchronous frequency
SSME	space shuttle main engine
VHM	vehicle health management

TECHNICAL MEMORANDUM

VEHICLE HEALTH MANAGEMENT USING ADAPTIVE TECHNIQUES— CDDF FINAL REPORT (No. 92-12)

I. INTRODUCTION

Vehicle health management (VHM) has become a term which has seen tremendous exposure during the last few years. The importance of VHM has always been emphasized, but its definition has remained enigmatic. A definition of VHM in this document is proposed in terms of mission success as:

> Vehicle health management encompasses all processes that have pertinent and positive effects on the success of a mission.

VHM includes all phases of a mission: preliminary design processes, design and test processes, qualification processes, prelaunch checkout, flight, and postflight checkout. VHM includes all disciplines: propulsion, electronics, structural, etc. A key aspect of VHM is automating manual operations tasks. Automation can be applied to all phases and disciplines of VHM, yielding tremendous savings in operational cost and reductions in operations time.

Automation can be implemented using classical methods, expert systems, or other types of techniques. This document summarizes Center Director's Discretionary Fund (CDDF) research that investigated automation techniques. Designs using a combination of cognitive computing methods are proposed and tested. A subsystem, space shuttle main engine (SSME) vibrational data analysis, is selected as the testbed.

II. PROBLEM STATEMENT

A. Selection of Test Case

In order to implement an automated system and to prove feasibility, a set of criteria was determined to select a system. These criteria were:

1. Real Case — The test should be based on real application, not simulation alone.

2. Human Knowledge Availability — There is existing human knowledge, or there are experts in the field.

3. Data Availability — Data is readily available for tests and verification.

4. Potential Benefits — Benefits can be realized in near future and can be proven to enhance present ways of doing business.

5. Feasibility — The task should not require inordinate cost and time.

After considering many candidate systems, SSME vibrational data analysis was selected. This system seemed to fit all criteria well. There is human expertise available, yet the expertise has been very difficult to document and to automate. A massive amount of engine data is available locally at NASA/Marshall Space Flight Center via computer network. Furthermore, automation of such tasks could result in significant reduction of manpower and time.

B. Space Shuttle Main Engine Diagnostics

1. <u>Background</u>. During the development of the SSME, significant progress has been made by both NASA and the aerospace communities in improving the diagnostic evaluation of high frequency dynamic data. Fast and reliable evaluation of such data is crucial to the space shuttle operations program for preventing catastrophic engine hardware failures; moreover, reliable diagnostic evaluations can extend scheduled maintenance intervals of major components such as the high-speed turbopumps. Dynamic assessment of the SSME is very challenging due to the computational and manpower intensive nature of the data acquisition and signal processing operations. Furthermore, the acquired dynamic signatures taken from various locations throughout the engine system can be very complex to analyze. Current SSME dynamic data processing and evaluation are performed postflight or following ground test with a typical diagnostic turnaround time of approximately 1 day. This primary evaluation can be improved upon significantly by automating manual analysis tasks.

One such task involves the evaluation of SSME high pressure oxygen turbopump (HPOTP) dynamic data for bearing distress frequency content. The primary failure mode for HPOTP bearings is uneven ball wear, and cage frequency is used to detect the characteristic bearing defect. Searching for the cage frequency content in high frequency dynamic test data is difficult due to the character of the SSME HPOTP dynamic environment as sensed by externally mounted transducers. Analysts must frequently contend with structural, combustion, and electronically generated noise which mask the cage indicators. Also, feedthroughs from the other three SSME turbopumps must be considered. When wear indication is observed by the externally mounted transducers, substantial ball wear has already taken place. Therefore, any indication of bearing cage or cage harmonic frequency content in SSME HPOTP dynamic data is justification for removing the unit from the flight inventory.

Spectrograms, commonly referred to as waterfall plots, are often used to detect cage frequencies in high frequency dynamic data channels. The cage frequency, along with subsequent harmonics, reflect nonuniform bearing rolling element diameters.[1] However, monitored HPOTP dynamic data channels frequently contain several other discrete and random narrow-band components which can coexist or mask predicted cage frequency signal content. Synchronous frequency (SF), i.e., fundamental rotor speed, and its harmonics along with structural and hydrodynamic signals contribute to the noise.

Decisions made by analysts are determined by their ability to distinguish anomalous cage frequencies. One key aspect of this effort is the use of analysts' cognitive knowledge. Locations of cage and synchronous frequencies, and their relations to the thrust level changes are understood by analysts based on the past experience. For example, an expert may look for cage frequencies without complicated numerical computations by simply scanning the hard copies.

2. <u>Preliminary Analysis</u>. After several interviews with analysts, it became obvious why automation of such processes is difficult to achieve. First of all, the analysts' decision may not be conclusive. The decision is often subjective, and at times there are differences in analysts' opinions. Furthermore, decision criteria have not been well established.

2

To further illustrate the decision process, two cases of actual engine data are presented. The first case is data with anomalous cage frequency as shown in figure 1, where the x and y axes denote frequency (in Hertz (Hz)) and time (in frame counts), respectively. In simplicity, the cage frequency determination can be linguistically described by an analyst as below:

Inspecting the plot at approximately 450 Hz, one can locate a series of very prominent peaks. These peaks are the representation of the SF. The 2C (second harmonic cage frequency) is found as a series of peaks between 390 to 410 Hz (approximately 2×0.43×SF).[2] As the thrust level changes, SF changes in proportion.
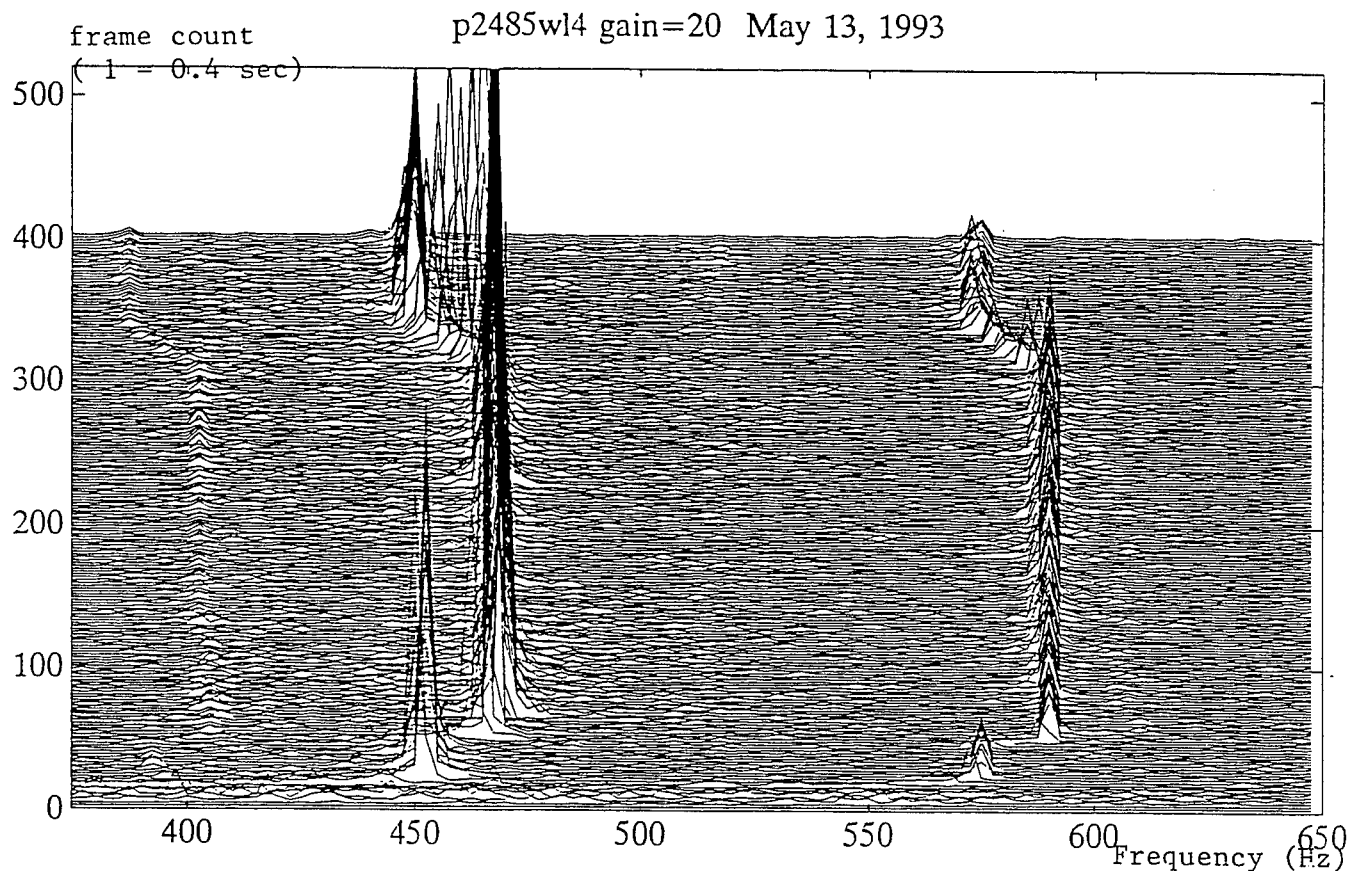
Figure 1. Anomalous case (2485wl45).

The second case, as shown in figure 2, is a nominal case. A similar procedure is used to determine its health. The SF is located and the cage frequency is searched for. Unlike the abnormal case, there are no consistent cage frequency peaks that vary with the SF. The same procedure is repeated to find the harmonics of the cage frequency. This case is found to have no anomalous peaks at any cage frequencies.

III. APPROACH AND METHODS

Further analysis of the human expertise allows a breakdown of the task into smaller and simpler sequential tasks as shown in figure 3.

3

p2495wl4 gain=20 May 13, 1993

Figure 2. Nominal case (2495wl45).

Convert Time Domain Data to Frequency Domain

Find Synchronous Frequency (SF)

Find Cage Frequencies (CF)

Detect Peaks

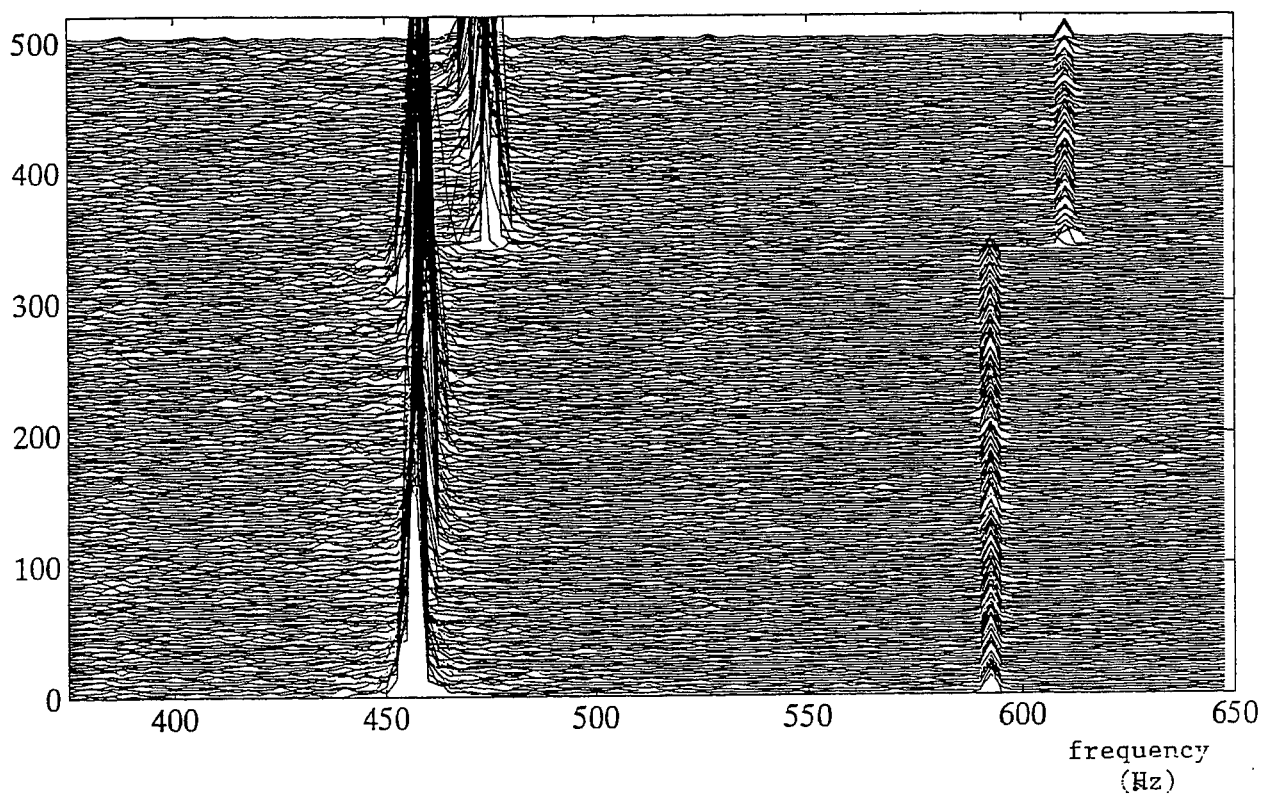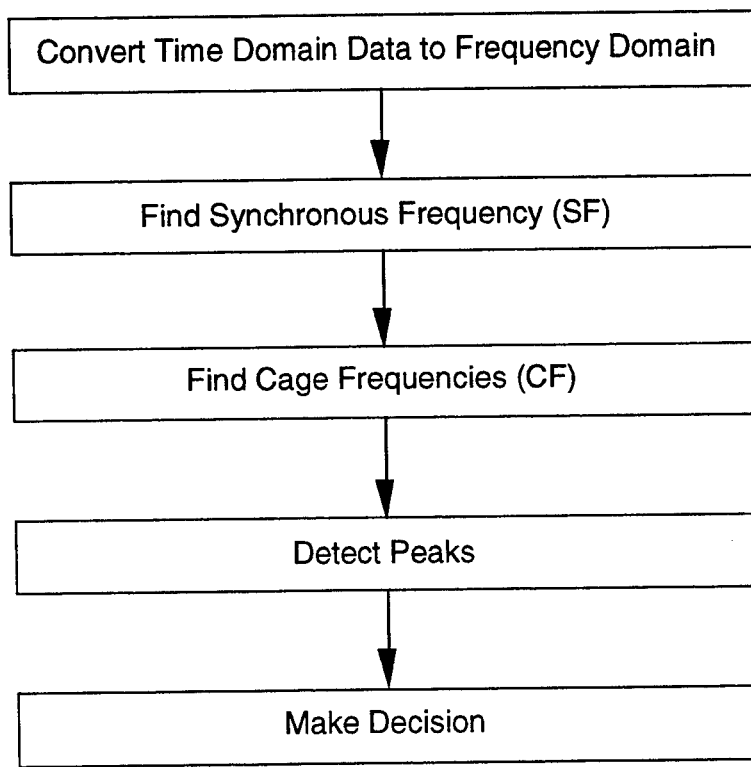Make Decision

Figure 3. Sequential breakdown of the expertise.

A. Discrete Fourier Transform

The discrete Fourier transform (DFT) defines the relationship between the time domain data and their representation in the frequency domain. The definition of the Fourier transform of a continuous signal $x(t)$ is defined as:

$$X(f) = F\{x(t)\} = \int_{-\infty}^{+\infty} x(t) \exp(-j2\pi ft)dt \ .$$

The inverse transform is defined as:

$$x(t) = F^{-1}\{X(f)\} = \int_{-\infty}^{+\infty} X(f) \exp(j2\pi ft)df \ .$$

These valuable relationships deal with continuous infinite length and infinitely many harmonically related complex exponentials. These relationships can be extended to sampled data. For a sequence of data that is uniformly sampled, DFT can be used efficiently. For DFT, the following equations are used:

$$\text{Analysis Equation: } X[k] = \sum_{n=0}^{N-1} x[n]W_N^{kn} \ ,$$

$$\text{Synthesis Equation: } x[n] = (1/N)\sum_{k=0}^{N-1} X[k]W_N^{-kn} \ ,$$

where

$$Wn = e^{-j(2\pi/N)} \ .$$

The relationship between frequency resolution, df, size of frame, N, and sampling frequency, dt, is defined as:

$$df = 1/(N \times dt)$$

Since the engine vibrational data are sampled at 10,240 Hz, in order to achieve $df = 2.5$ Hz, the frame size, N, is set to 4,096.

B. Determination of Synchronous Frequency

The SF plays a very important role since cage frequencies are located based on SF. Since the SF is the most prominent set of peaks, one way to find the SF is to look for the maximum. However, typical cases have shown that the problem is not this simplistic. Two problems arose: (1) due to discretization error, the SF seemed to fluctuate about the expected value; and (2) in some cases, SF does not manifest itself for a duration of time due to very high noise level, lack of synchronous response (i.e., very quiet pump), or a combination of both. The two problems mentioned above are illustrated in figure 4.
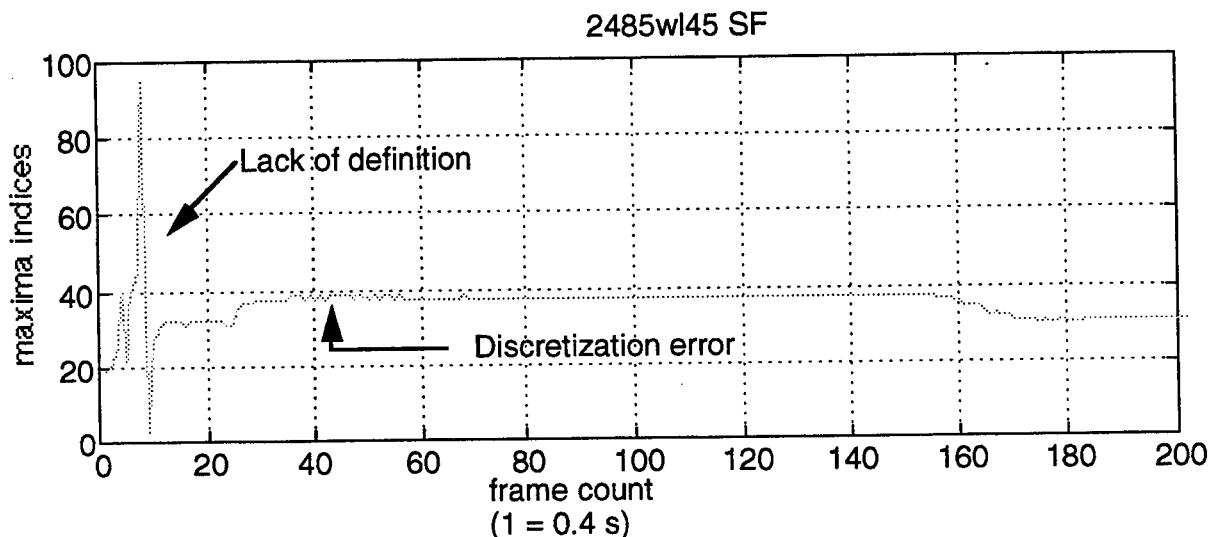
Figure 4. Typical error in finding SF.

Discretization errors, which are often manifested as small transient peaks, can be minimized by using various digital filters, for example, averaging or the Butterworth low pass filter.

For the second case, as shown in figure 5, when the SF is not well defined, further investigation is needed. Figure 5 displays the first 20 frames of 2485wl45. The SF is not well established in the first 10 frames, thus creating incorrect maximum indices. One method of dealing with the lack of definition is to ignore the engine data until an obvious SF is found. This method can be used only if it is assured that SF is found for most of the cases. This "ignore-if-not-sure method" was not considered since loss of information may be too great when SF is not manifested for a significant duration. An alternate set of algorithms is investigated to deal with the ill-defined area. Two of such algorithms take into consideration the analysts' a priori knowledge on the SF: credibility and correlation.

1. Credibility Filter. The first approach deals with the credibility of a data point using a simple credibility filter. A set of credibility filters is constructed based on the analysts' experiences. A set of trapezoid filters is generated. The center of the trapezoid filter is defined by a priori knowledge. As a data point falls away from the center, the data point becomes less credible. As the data point gets closer to the mean, the better credibility the data point will have. A series of trapezoid credibility filters were defined as shown in figure 6.

The credibility is defined as follows:

$$CR = \begin{cases} 1.0 & \text{if ABS(mean–data)} \quad =< \quad 0.1\ W \\ 0.0 & \text{if ABS(mean–data)} \quad > \quad 0.5\ W \\ 1-(5/2\ W)(\text{ABS(mean–data)} -0.1\ W) & \text{otherwise} \end{cases}$$

where W is the width of the filter, mean is the mean of the filter, and ABS is absolute value.

Using a previous model, a set of predicted SF is calculated based on the thrust level schedule (fig. 7). The predicted SF is used to construct a series of credibility filters as shown in figure 8.
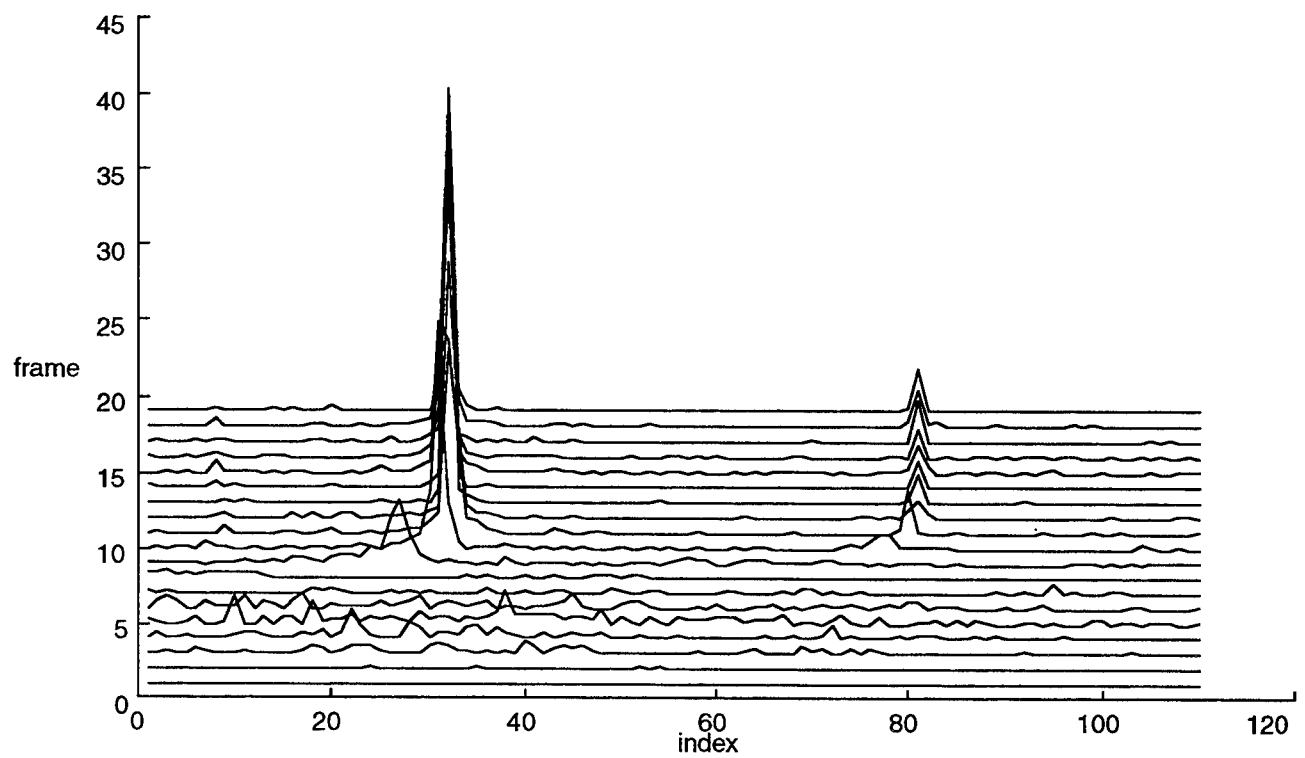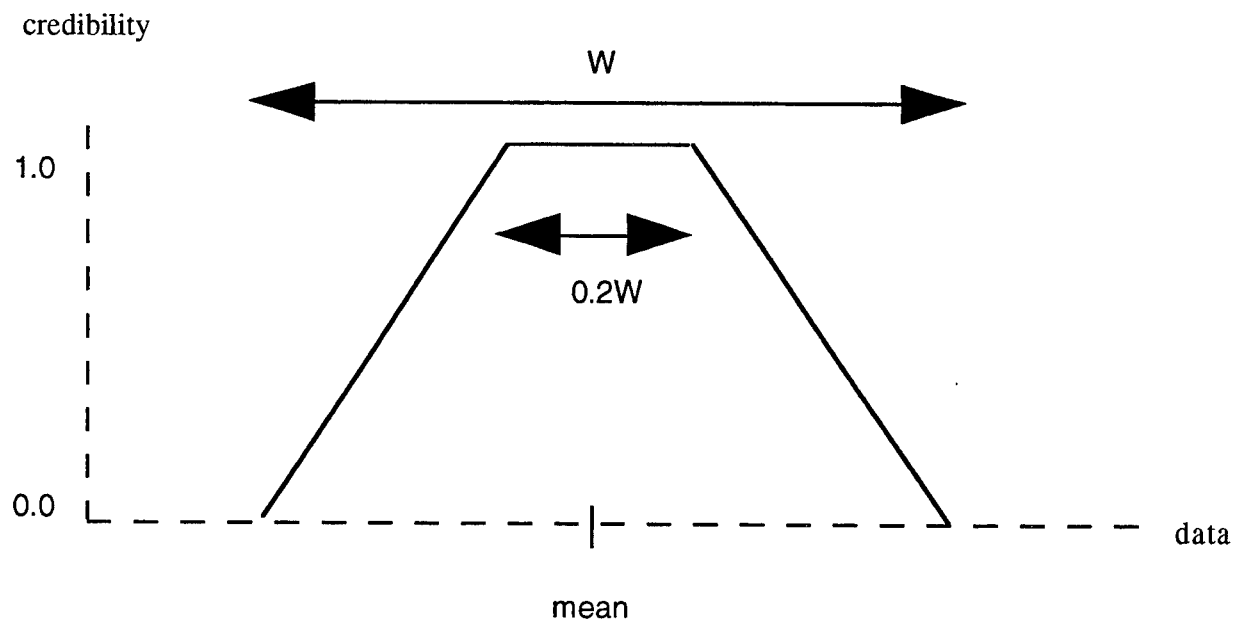
Figure 5. Ill-defined SF (2485wl45).
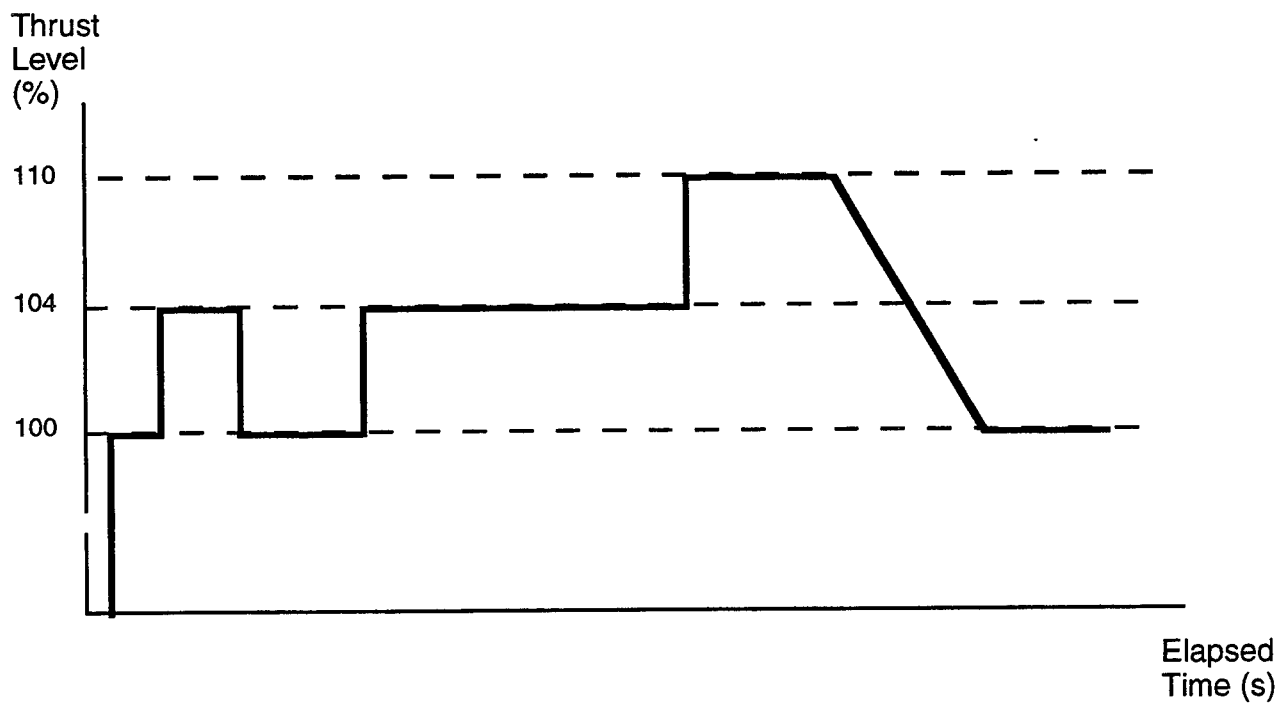

Figure 6. Credibility filter.

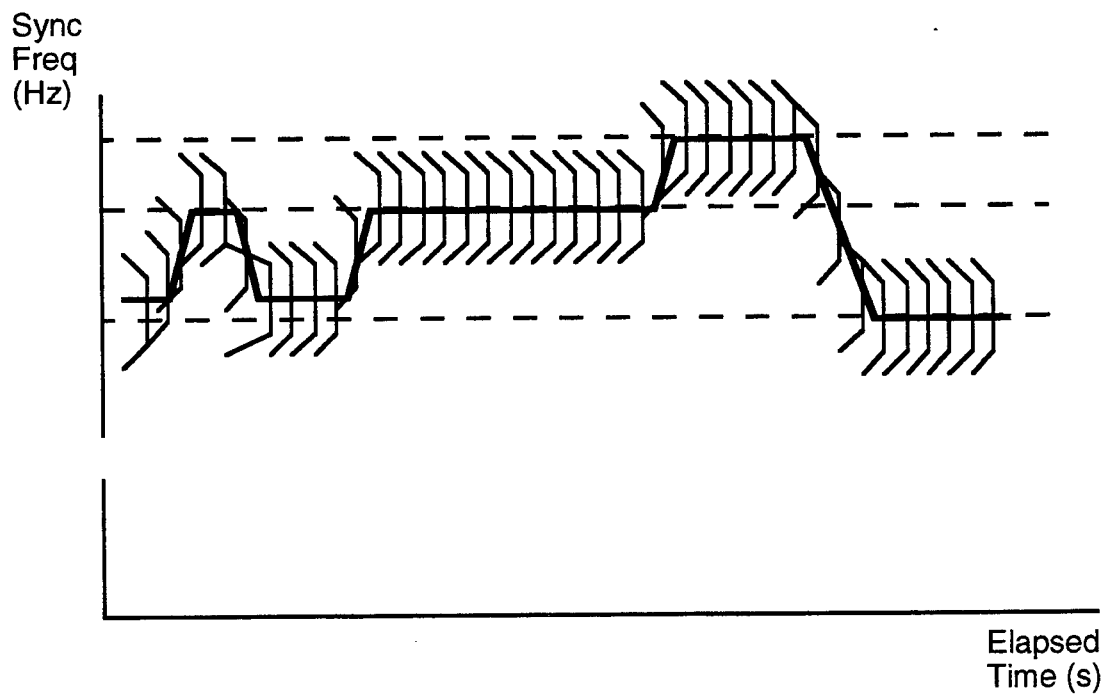Figure 7. Example of thrust level changes.

Figure 8. Two-dimensional credibility filter with moving mean.

8

After the credibility of each data point is determined, a simple rule is implemented: the less credible a data point is, the more important the a priori information is. As the data point becomes more credible, the less dominant the a priori knowledge is. This rule implementation is illustrated as figure 9.
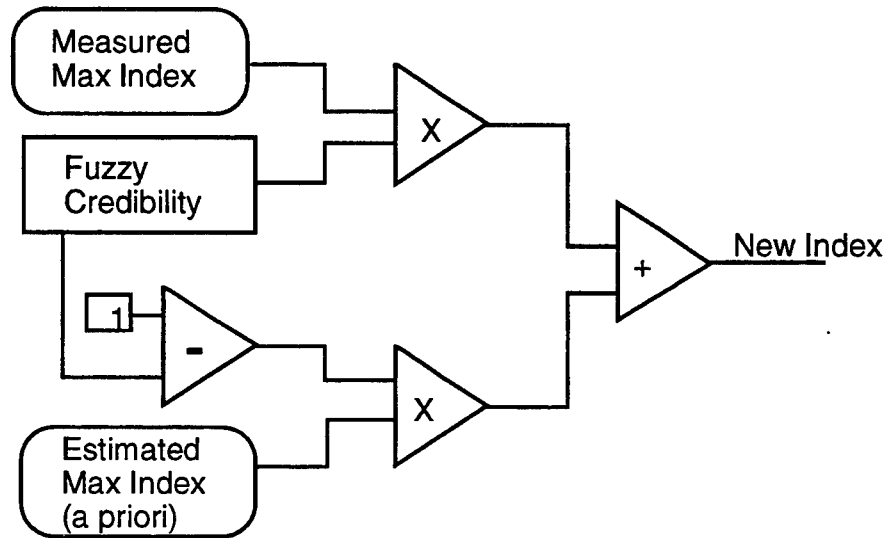

Figure 9. Credibility implementation.

Using the credibility filter with $W = 10$, the results are as shown in figure 10. It seemed that the level of the high pressure fuel pump was as high as the SF such that maxima found fluctuated between the level of SF and the high pressure fuel pump. Figure 10 illustrates a case where a credibility filter effectively eliminated erroneous information. Figure 10a is a plot of maxima as found. By comparing against the expected SF, a credibility plot is generated as shown in figure 10c. Finally a new set of SF is found. The absolute value of the difference between the expected values and the processed values is shown in figure 10e.

Even though the credibility filters were effective for many of the cases, some data files resulted in less than satisfactory results. Two factors contributed to the poor results. One reason was a linear model that deviated significantly from the actual data. It seemed that the linear model to calculate the center of the trapezoid filter was not accurate. This model error resulted in low credibility, thus causing a large compensation in the SF level, which became another source of error. Another drawback in the credibility filter was its inability to remove discretization error. Discretization error, which is manifested in the form of small transient noise, maps onto an approximately equal credibility value as the noiseless signal. In order to minimize this type of erroneous reasoning, more elaborate decision criteria had to be implemented.

2 . Correlation. The second approach to find SF considered an overall shape of the expected SF and the found SF. Pearson's[3] r is used to determine the correlation between the found SF and the expected SF. If linear correlation exists, then a new SF is generated based on the expected SF and the actual data (fig. 11).

9
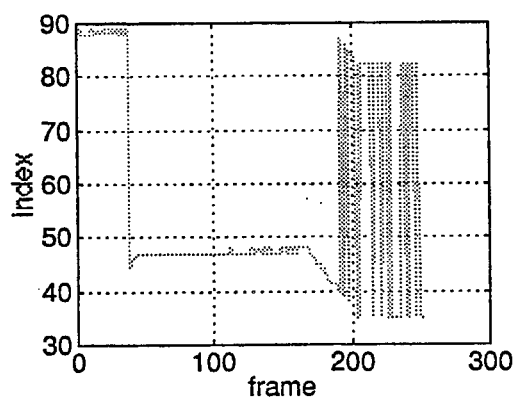
(a) Raw maxima found
(1595ht135)

(b) Expected SF

after fuzzy filter
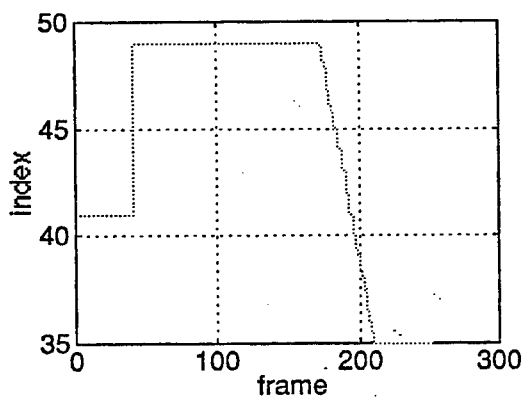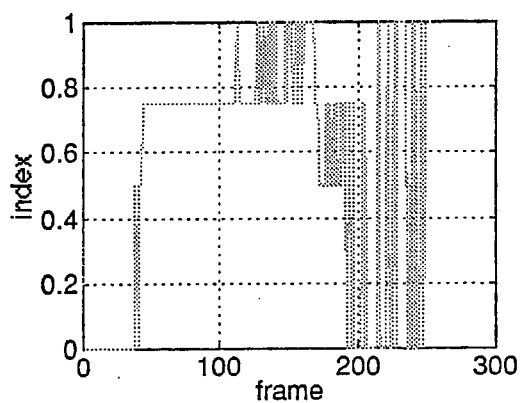
(c) Credibility Rate of Maxima
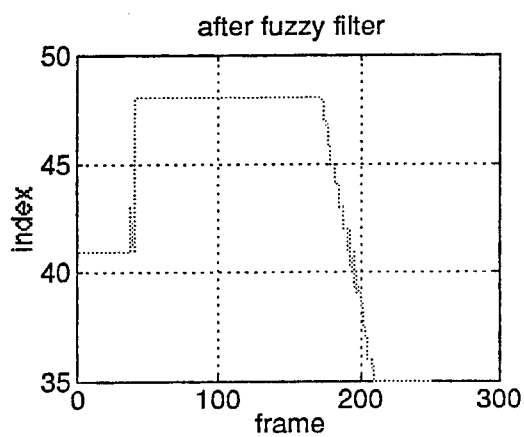
(d) SF after processing
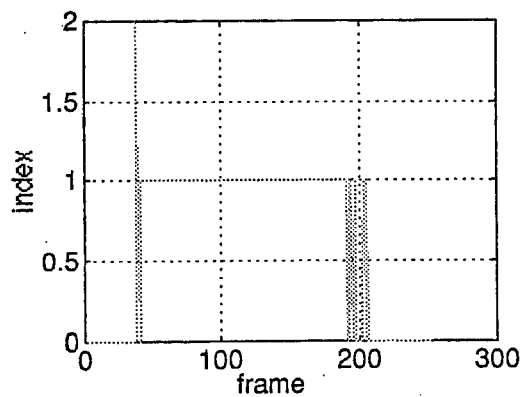
(e) abs(expected SF - processed SF)

Figure 10. Credibility filter results.

10
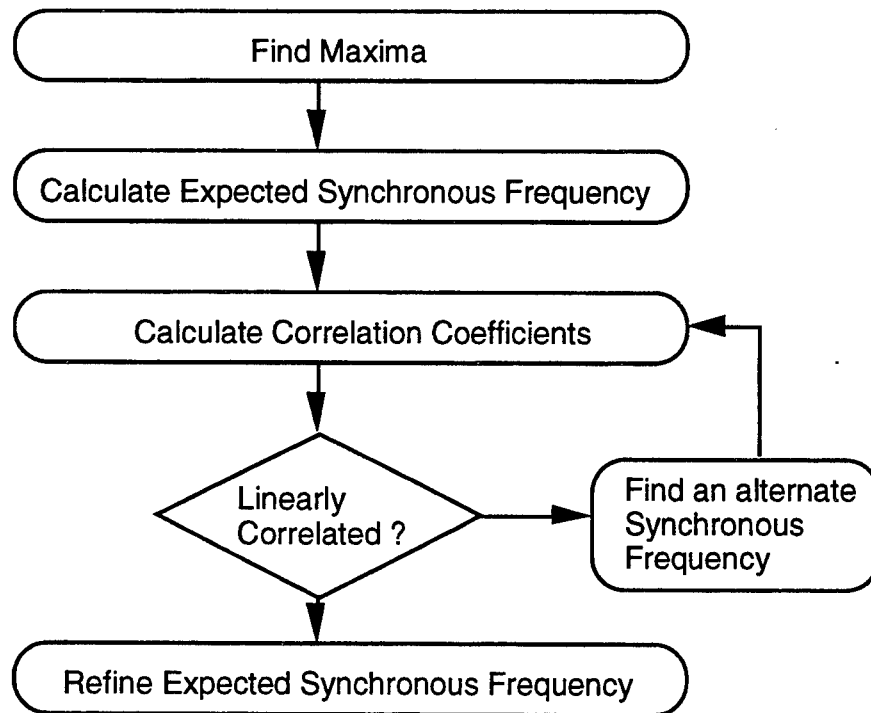
Figure 11. Flowchart: SF using correlation.

By use of Pearson's[3] r coefficient, correlation coefficients of two sets of parameters are found (see equation 2.1 of reference 4). Its linear correlation threshold (fig. 12) varies with the sample size. For a set of data pairs, $\{(x,y)\}$, whose mean and standard deviations are μ and σ respectively, Pearson's r is defined as:

$$r = \sum_{i=1}^{N} \frac{(\mu_x - x_i)(\mu_y - y_i)}{\sigma_x \sigma_y N}$$

(equation 2.1 of ref. 4)
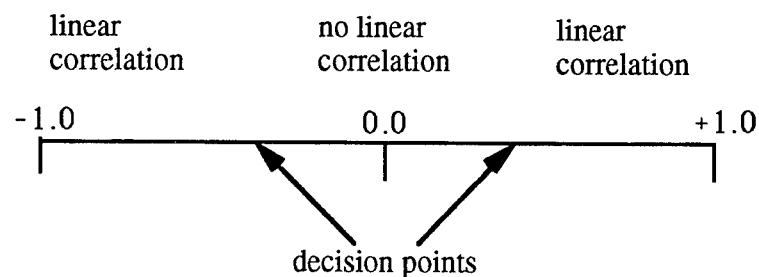
Figure 12. Linear correlation regions.

Decision points are given in absolute values, and the value is inversely related to the size of samples. An example is given in table 1.[4] For example, with the sample size of 100, the decision points are ± 0.196 with 95 percent confidence.[3]

Table 1. A guide to use Pearson's[3] r coefficient.[4]

Sample Size	Decision Pt	Sample Size	Decision Pt	Sample Size	Decision Pt
5	0.878	20	0.444	80	0.220
10	0.632	50	0.279	100	0.196

An algorithm to use the correlation coefficients is described as follows:

1. Find potential SF by using maxima function.

2. Compare the found SF against the thrust level schedule.

3. If they are not linearly correlated, use alternate methods (such as credibility filters, etc.). If the found SF and expected SF are linearly correlated, then find a coefficient using equation (2.2).

$$k = \frac{1}{N}\sum_{i=1}^{N}\frac{L_{f(i)}}{L_{e(i)}}$$
(Equation 2.2)

where $L_{f(i)}$ is the ith thrust level found $L_{e(i)}$ is the ith expected thrust level.

4. Multiply k to the expected thrust level to acquire a new SF.

Figure 13 illustrates the process described previously. The first is the found SF. The expected SF shows two constant thrust levels. When the found SF and the expected SF are found to be linearly correlated, then the average value, k, is derived using the equation (2.2). The value, k, is then multiplied to the expected SF to generate the new SF.
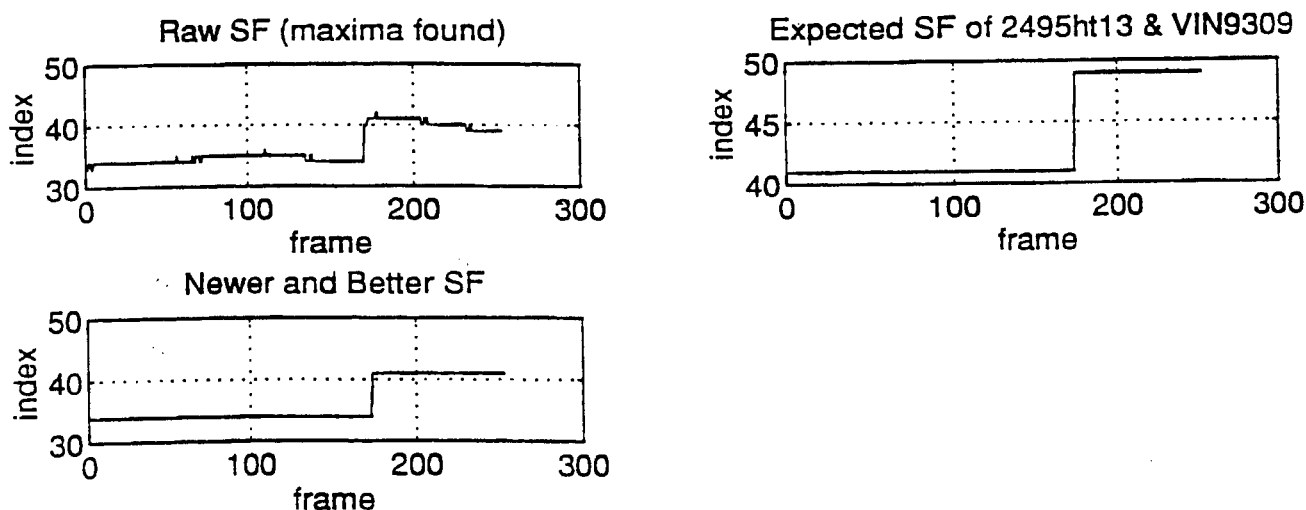
Figure 13. Correlation coefficients results (2495ht135).

This method is simple to implement, and it proved to be less noisy than the credibility method. Effectiveness of this algorithm is due to the fact that correlation deals in terms of similarity in shape. Therefore, even when the numerical values of SF are not accurately predicted, the overall shape of the predicted SF can be used to generate a clean SF.

C. Cage Frequencies

The approximate location of the second harmonic cage, $2C$, frequency is found by multiplying the SF by a factor of 0.86 (= 2×0.43). In most cases, up to $7C$ can be investigated. For simplicity, $2C$ and $3C$ are included in each file for testing. Since the SF is determined in terms of indices as described in section B.2, chapter II, cage frequencies are derived in terms of indices as follows:

Definition:
SF_i as the index of SF,
$2C_i$ as the index of 2C,
$3C_i$ as the index of 3C,
StF as the start frequency of a data file in Hz,
SF as the synchronous frequency in Hz,
df as the frequency resolution in Hz,
$2C$, $3C$ as the two times and three times the cage frequencies respectively in Hz.
The first index is 1.

Frequency index, F_i, can be expressed in terms of frequency, F, and StF,

$$F = (F_i-1) \times df + StF \tag{1}$$

By definition,

$$2C = 2 \times 0.43 \times SF$$

substituting in SF using equation (1),

$$= 0.86 \times ((SF_i-1) \times df + StF) \tag{2}$$

Then $2C_i = (2C-StF)/df+1$, substituting in equation (2),

$$= 1/df \times (0.86((SF_i-1) \times df + StF) - StF) + 1$$

$$= 0.86 SF_i - (1-0.86)/df \times StF - 0.86 + 1$$

$$= 0.86 SF_i - 0.14/df \times StF + 0.14 \tag{3}$$

By the same method, $3C_i = 3 \times 0.43 \times SF$ reduces to

$$= 1.29 \times SF_i + 0.29/df \times StF - 1.29 + 1 \quad . \tag{4}$$

Actual values of $2C_i$ and $3C_i$ are the closest integers to the calculated values. For example, if a file starts at 375 Hz, where the index is 1, and SF_i is determined to be 35 (or 460 Hz) with the frequency resolution is 2.5 Hz, then

$$2C_i = 9 \qquad (\text{or } 395 \text{ Hz}),$$

$$3C_i = 89 \qquad (\text{or } 595 \text{ Hz}).$$

Using equations (3) and (4), locations of the expected $2C$ and $3C$ are found as shown in figure 14.
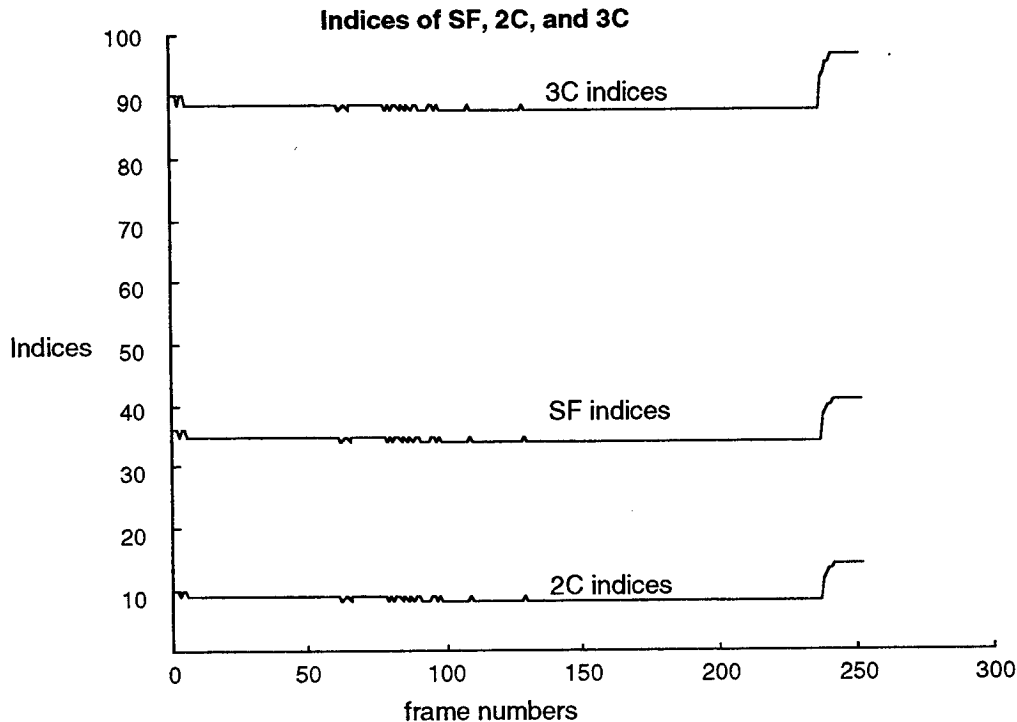
Figure 14. 446ht45 *SF*, and expected *2C/3C* indices (raw data without filtering).

D. Anomaly Detection

1. <u>ANN Approach</u>. To detect anomalous peaks, artificial neural networks (ANN) are developed. Various configurations are considered to optimize the design.

Several tests using various ANN configurations were performed to find an optimal configuration. Most of the tested cases used a frequency resolution of 2.5 Hz since this frequency resolution value is most often used by analysts. One case used the 1.25 Hz case. For the neural network training, MatLab™ (MathWorks, Inc.) and NETS™ (NASA Johnson Space Center) were used. Both of these software tools utilize the back-propagation algorithm for training.

1.1. Initial Training and Propagation Results. The input to the ANN was 13 points centered about the expected cage frequency. To generate a training set for the neural networks, two approaches were considered. The first approach was to make manual decision on each individual frame of a data file. This approach was done by manually examining each frame of data to see if an

14

obvious anomaly existed. Understandably, this approach required considerable manpower and patience to generate a sufficiently large training set. This approach involved manually labeling normal and abnormal frames. First of all, an abnormal data file, 2485PB45, was chosen. The file was normalized between zero and one, and the decision was manually made by a human operator on each frame. The decision assignment was 0.9 for nominal and 0.1 for anomalous frame. This task was quite subjective, and at times proved to be very difficult to determine its assignment. There were many cases where the decision of anomalous/nominal was very difficult. However, it was assumed that if "enough good information" is given to the neural network, the network should be able to learn the desired patterns. A total of 207 frames were individually evaluated and tagged. Seven artificial sets were added to accentuate the importance of the middle of the frame. Over all, the training file included 149 anomalous frames and 58 nominal frames. The neural network consisted of 13 input neurons, 8 hidden layer neurons, and 1 output neuron. After several iterations, the root-mean-square (RMS) error was reduced to 0.11, and the training was halted. The training set was used to verify the learning. The results were almost inconceivable. Out of 207 frames, there were only 2 errors. This accurate mapping seemed surprisingly good due to the subjective nature of the manual decisions. However, good training did not seem to translate to a better design. When tested using other files, this network failed. It seems that the network has learned some specific idiosyncrasies about the training set, and the learned behavior was not able to generalize. This conclusion was verified further by reexamining the training file. One of the artificial frames was mistakenly labeled wrong, and the neural network mapped this frame just as it was trained. This ability to converge to the training set was impressive, but the lack of generalization was of serious concern. More tests will be required to characterize this behavior using larger sets of training data.

The second approach was to select one data file with nominal data and another data file containing anomalies. Then each file is tagged as normal (0.9) and abnormal (0.1). The objective of this approach was to see if the ANN could learn by itself the inherent distinction between normal and abnormal cases. This approach to labeling each data file as a whole must contain "enough amount of good information." On many occasions, the cage frequencies do not appear for the full duration of the test. Therefore, a subjective decision should be made whether a file includes "enough" good information.

A file, 2474wld0, was used to propagate and to test the trained network using the file labeling. The file included 13 points centered at the calculated cage frequencies ($2C$ and $3C$). The 13 points were normalized such that the lowest value was set to 0, the highest 1. When the data were propagated, the results seemed to be inaccurate. Defining the correct response to be less than 0.2, out of 250 frames, the ANN found 3 hits for $2C$ case, and 10 hits for $3C$. It was hypothesized that the reason for the low hits was due to the skewing of the peaks. Each data set was shifted left one at a time, and 0.5 was added as the 13th element. Table 2 lists the results compiled with shifting.

Table 2. Network testing with shifts.

	2C	3C
shift left 0	3	10
shift left 1	3	28
shift left 2	34	15
shift left 3	4	N/A

It became apparent that the trained network was very sensitive about the position of the peaks. Two techniques were proposed to enhance better results:

1. Shift and propagate

2. Peak detection using three points.

These two methods bear a similarity in that consistency of peaks, and not the exact location, is sought. As long as there are peaks at the same frequency location, the network would work well regardless whether the location of the peak is 410 Hz or 412.5 Hz.

1.2. Artificial Neural Network Design

a. Shift and Propagate. A network with 13 input nodes with varying sizes of a hidden layer is trained with two 1.25-Hz files: 2485wl45 (anomalous) and 2495wl45 (nominal). For testing, 21 normalized points were selected from each spectral frame centered at the expected frequency. First, 13 points were entered into the trained network for propagation. Then the 21-point data set is shifted left, and 13 points are again input to the trained network. This continues until the last 13 points of the set are used for propagation (fig. 15).
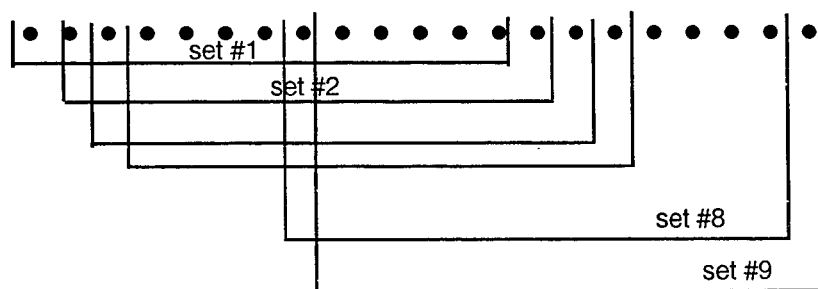
Figure 15. Shifted input data sets.

The number of hidden nodes was arbitrarily changed from zero to six. This "shift and propagate" method generated 13 outputs per input frame. At the end of each file, all shifts, zero to eight shifts, are compared and then the maximum number of anomaly detection was recorded. Then a decision is made whether the data had anomalous characteristics. A network with no hidden layer seemed to work the best. The synaptic weights are given in table 3.

Table 3. ANN No. 1 neuron weights (bias = 3.4).

#	1	2	3	4	5	6	7	8	9	10	11	12	13
	–15.3	–10.4	–22.3	–5.8	–10.5	–6.2	+14.1	+3.3	+3.2	+4.6	–10.0	–22.2	–12.3

Table 4 delineates the results using this neural network. The last column represents an analyst's opinion. The ANN performed well except in the engine files on 446. The analyst believed that there was a very probable anomaly, but the neural networks show nominal condition. The analyst's decision, it turns out, was based on $3C$ (three times cage frequency) information, and the neural net was propagated using only the $2C$ data. This fact necessitated enhancement to include other cage harmonics.

16

Table 4. ANN No. 1 results (shift and propagate).

File Name	ANN Recognition	ANN Decision	Analyst's Decision*
1595ht135 1595pb45 1595wl45	23 11 5	max = 23,	2
1675ht135 1675pb45 1675wl45	8 8 34	max = 34,	2
2485ht135 2485pb45 2485wl45 (train)	34 35 78	max = 78,	5
2495ht135 2495pb45 2495wl45 (train)	6 12 5	max = 12,	0
446ht135 446pb45 446wl45 446wld0	5 6 5 5	max = 12,	3 (see 3C case)
449ht135 449pb45 449wl45	6 9 23	max = 23,	4

* Note: Analyst's decision is denoted 0 to 5, where 0 represents normal data and 5 represents highly recognizable anomaly.

b. Rotate and Propagate. An artificial neural network with 13 input neurons, 8 hidden layer neurons, and 1 output neuron was trained with two 2.5-Hz files: 446ht13L (anomalous) and 2495ht13L (nominal). These two files are generated using the Pearson's r and linearization technique as described in section III.B.2. Then the 3C file from 446ht13 was used for consistent peaks (figs. 16 and 17).

The training was done using back propagation with various learning rates. The output assignments were 0.1 for the nominal case and 0.9 for the anomalous case. The first training set consisted of the above two files appended consecutively. Each file contained 252 timeframes with normalized magnitude to have the maximum magnitude of 1 and minimum of 0. Training a neural network involves fairly mundane tasks of selecting transfer functions, hidden layers, transfer functions, etc. Various learning rates were used ranging from 1 to 0.001. High learning rates seemed to incur rapid changes, usually resulting in fluctuations, but overall error did not seem to get smaller. It seemed that a learning rate of 0.01 allowed a reasonable training point. The transfer function used for this training was the log-sigmoid function (figs. 18, 19, 20).

The summed squared error seemed to have a steady decline for the first 300 epochs. One aspect of the learning rates was of concern. If the neural network was presented with 252 of the anomalous frames first, would the network prematurely converge before nominal data can be presented?
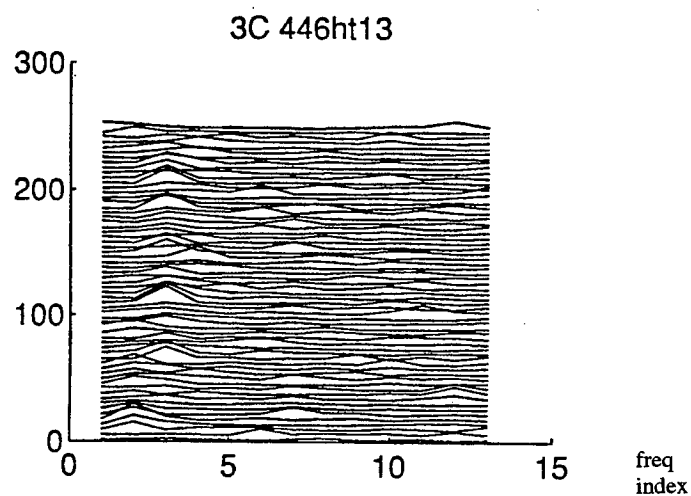
17

frame count
(1 frame = 0.4s)

3C 446ht13

Figure 16. Anomalous file (446ht13L) for training.

frame count
(1 frame = 0.4s)

2C 2495ht13 from CredibleSF1
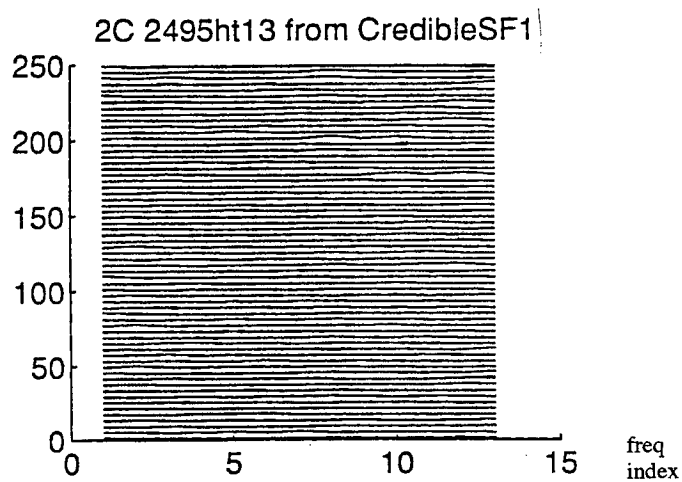
Figure 17. Nominal file (2495ht13L) for training.

18
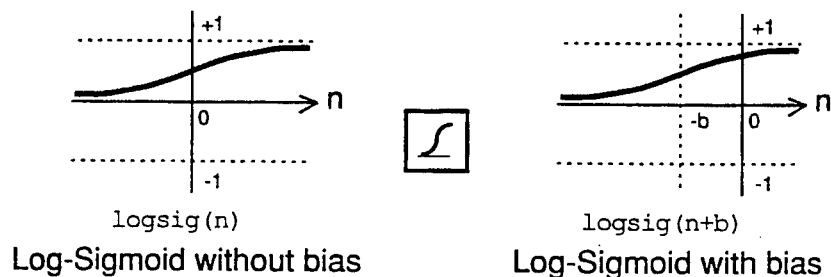
Figure 18. Log-sigmoid transfer function.
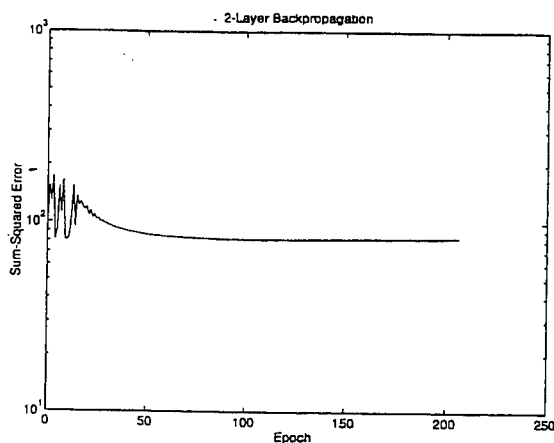
Figure 19. Learning rate = 1.
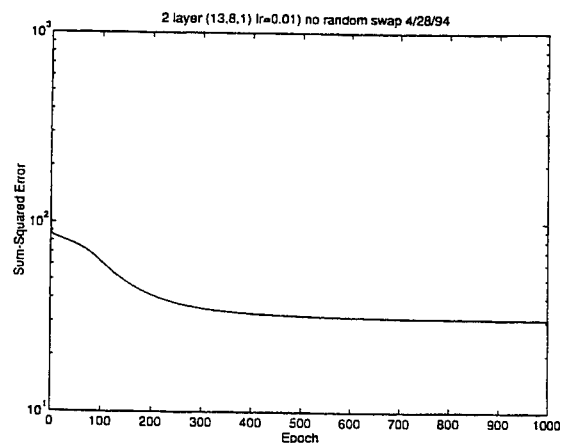
Figure 20. Learning rate = 0.01.

Would a mixed training set perform better? With these questions in mind, 400 out of 504 frames were randomly selected and swapped. Using the same learning rate of 0.01, a new learning rate was performed. There was a faster reduction of summed squared error using the randomly swapped input file. And at 1,000 epochs, the error was reduced to approximately 250, as opposed to over 300 for the nonswapped case. After 2,000 epochs the training stopped (figs. 21 and 22) (see appendix A for the weights and biases).
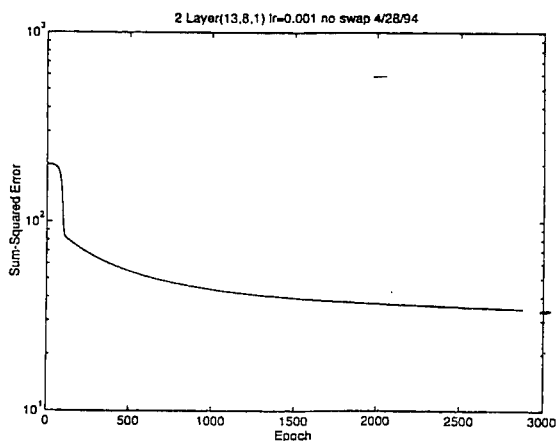
Figure 21. Sequential training.
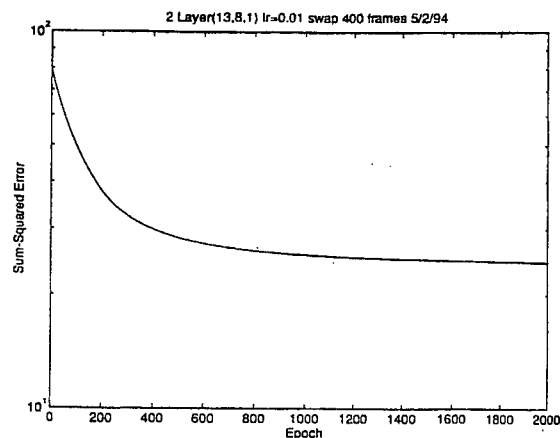
Figure 22. Alternate training.

19

A hit is defined to be a propagated value greater than or equal to 8.5 and less than 9.5. Initial propagations indicated that the network was very sensitive to the magnitude and location of the peaks. For example, when raw data are propagated without normalization, there were zero hits. Also when the peaks were shifted, the results were less than satisfactory. Using these observations, all data sets were scaled such that the maximum number in the file would be 1.0. In addition, the 13 data points were rotated and propagated to find consistent peaks (fig. 23). The results are summarized in the table 5.
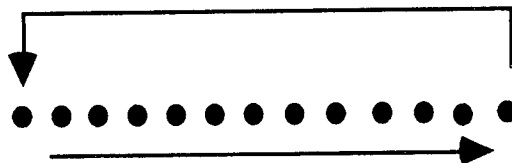
Figure 23. Rotate and propagate.

Table 5. Rotate and propagate.

| File Name	ANN 2C Hits	ANN 3C Hits	ANN Decision	Experts Decision*
1595pb45	21	37		
1595wl45	20	50	max = 21,50	2
1675ht135	17	13		
1675pb45	5	21		
1675wl45	34	34	max = 34, 34	2
2495ht135l :Training Set	14	148		
2495pb45	11	105		
2495wl45	19	164	max = 19,148	0
446ht135 :Training Set	14	123		
446pb45	19	29		
446wl45	11	92		
446wld0	26	17	max = 26,123	3

* Note: The expert's decision is denoted by 0 to 5, where 0 represents normal data and 5 represents a highly recognizable anomaly.

Inspection of the results, as shown in table 5, seemed to indicate a correlation between the peaks and the hits. A high number of hits represent a consistent series of peaks. The files on test 2495 included a high number of hits in the 3C area. These hits were later identified by experts as the high pressure fuel pump peaks. The neural net was able to recognize peaks, but the network could not make a distinction between the 3C and other similar peaks. Further investigation is needed to find a better solution to this problem.

c. Peak Detector. This peak detector design utilizes an assumption that a definition of "peak" can be taught to the artificial neural network. In order to achieve this learning rate, two files,

20

2485wl45 and 2495wl45, were used. Instead of providing 13 points, the peak detector network was provided with 10 frames of 3 points from the two files. If there was an anomaly, the peak would appear consistently at the second (or middle) point of each frame (fig. 24). In addition to the purely geometric definition of a peak, by providing 10 frames of data, the neural net was to learn about subtleties of temporal relationships between frames.

frame #1   frame #2   frame #9   frame #10

Figure 24. Peak detection using 10 frames.

The results using the peak detector seemed accurate. For 2473wl0, the 2C area was believed to be a 60-Hz line noise harmonic. This belief is based on the fact that the 60-Hz harmonic is independent of the thrust level changes. Thus, as the thrust level changes, the 60-Hz harmonic will not fluctuate. Since the neural network was not trained to differentiate this case, the network recognized the 60-Hz harmonic as 2C. However, the network correctly recognized 3C data. Based on these findings, the engine was found to have cage frequencies by the network as was the case by the experts. Table 6 delineates the results. Under 2C and 3C columns, most likely cage frequency values are listed. Under No. of Hits, the number of hits of the corresponding frequencies are listed.

Table 6. Peak detector.

File	2C	No. of Hits	3C	No. of Hits	ANN	Expert*
1595ht135	420	30	None		Y	2
1675wl45	400 (398)	77 (48)	None		Y	2
2473wl0	418 (420)	63 (121)	625	58	Y	4
2485wl45	403	110	None		Y	5
2495wl45	None		593	167	N	0
446wld0	393	32	588	40	Y	3
449wl45	408	42	610	36	Y	4

* Note: 0 indicates normal, and 5 indicated obvious abnormalities.

As was in the case of rotate-and-propagate, file 2495wl45 seemed to have consistent peaks at 593 Hz, which is the high pressure fuel synchronous feedthrough. The artificial neural network parameters are listed in appendix A.

2. Discussion of Results. Understanding results from an artificial neural network may be a difficult task, but a necessary one if this network is to be used in a real environment. It may be almost impossible to understand the full spectrum of ANN capabilities and limitations, but in this section, an attempt was made to discover the capabilities of the trained artificial neural network.

This implementation of the statistical maxima detection involves algebraic count of the maxima at each index. This technique verified that the trained network was indeed sensitive to the location of the peaks. Figure 25 is a nominal case without cage frequencies. The statistical distribution has minimal fluctuation. On the other hand, figure 26 is an anomalous case.
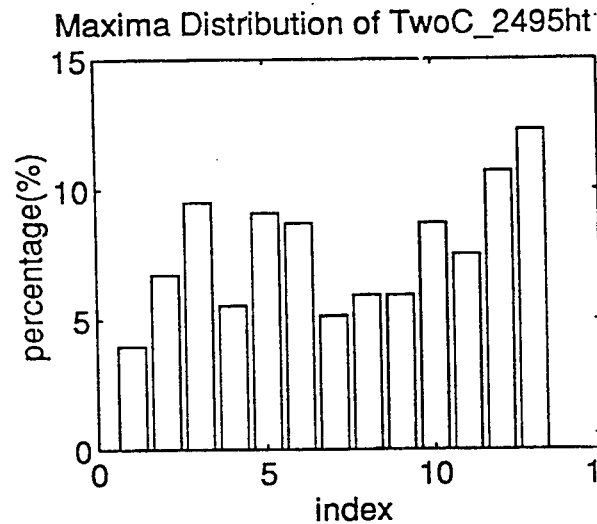
Maxima Distribution of TwoC_2495ht

Figure 25. Statistical distribution of nominal case (2495ht135:2C).

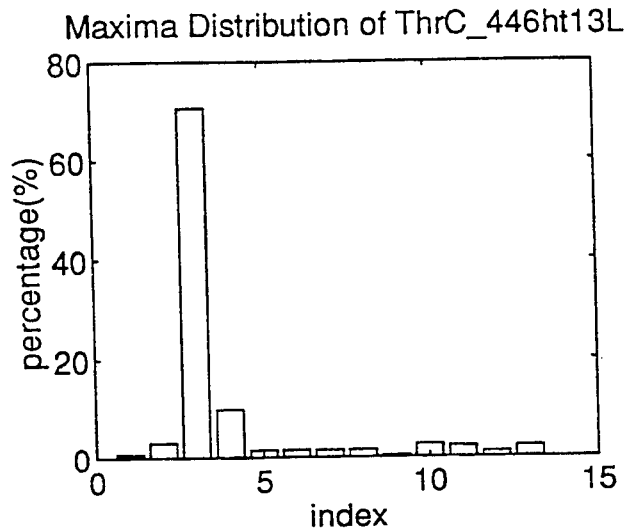## Maxima Distribution of ThrC_446ht13L

Figure 26. Statistical distribution of anomalous case (446ht135:3C).

This technique could be further developed into another tool for determining anomalies within the engine. The underlying hypothesis is that the noise floor is white. In laymen's term, a probability of an occurrence of a peak at one frequency is equal at any frequency. If cage frequencies do not exist, then the maxima found in the 13-point data file should not exhibit any prominence at one frequency. If cage does exist, then the maxima found should be located at or near a specific index. One very attractive property of this algorithm is its simplicity. Its simplicity renders itself to easy algorithm development and verification. More results are provided in appendix C.

IV. CONCLUSIONS

Cognitive computing techniques (CCT), such as analog logic and artificial neural networks (ANN), were effectively utilized to model the decision process to detect anomalous cage frequencies. Analog logic was used to model knowledge that could be expressed in terms of linguistic terms, e.g., near, close, etc. Pearson's r was used to determine the correlation between the expected values

22

and the found values. ANN's were used to define anomalous peaks in the spectral domain. Several configurations of artificial neural networks were tested and documented. CCT seemed to offer overall results that were similar to the analyst's manual decisions.

Despite the promising results to assimilate the manual decision, there were some concerns that were manifested in the research. Most of the concerns were originated from the use of ANN's during training and propagating (posttraining). Training an ANN involved selecting many variables such as learning rates, the number of hidden layers, the number of hidden nodes, etc. These parameters affected the convergence and success, and many trials were needed to find an effective configuration. Even after a network is successfully trained, as described in section D.1.1, the trained network failed when tested with a new set of data.

The self-learning capability of ANN is a double-edged sword: ANN can learn complex mappings by itself, but such a system cannot be verified easily. The internal structure, which has features of parallel processing, is very complicated to analyze. This inscrutability of ANN is a major obstacle if an ANN system is to be used in a dynamic environment. However, understanding these aspects of ANN, a system could be designed to utilize ANN's parallel processing and real-time capabilities. A system designer can overlay a supervisory module to detect the output of the neural networks such that no adverse action is taken by ANN alone. In addition, imposing explicit limitations on the ANN, e.g., peak detection rather than anomaly detection as done in this research, may simplify verification processes.

There are many features that make CCT suitable for automation of manual tasks. CCT allows easier translation of human knowledge to computerized automation. Analog logic allows direct translation of linguistic expression to quantitative numbers. ANN's can be implemented to optimize its self-learning capabilities without explicit instructions. ANN can be especially beneficial when human knowledge is difficult to be articulated.

Based on this research, the following tasks are proposed to be investigated further:

- In order to make an automated system, a more advanced type of decision algorithm is required to take into account the intensity of the peaks, discrimination of line noise from abnormal data, and past experiences.

- Better definition of 60-Hz data and other pertinent information, such as fuel pump data, should be given to the neural networks so that cage can be discriminated from other irrelevant data.

- Develop the system on a hardware platform using digital signal processors (DSP's), artificial neural net chips, and fuzzy logic chips. This hardware implementation would allow real-time processing. This hardware implementation task proposal has been submitted for code C funding.

One useful by-product of the research was preprocessor software. Based on a graphical user interface, the preprocessor allows the user to perform simple filter functions, data displays, fuzzy filter generation, and file input/output. In addition, this software can be used to view data, in time and frequency domain, in two or three dimensions. A typical display of the preprocessor is shown in figure 27.
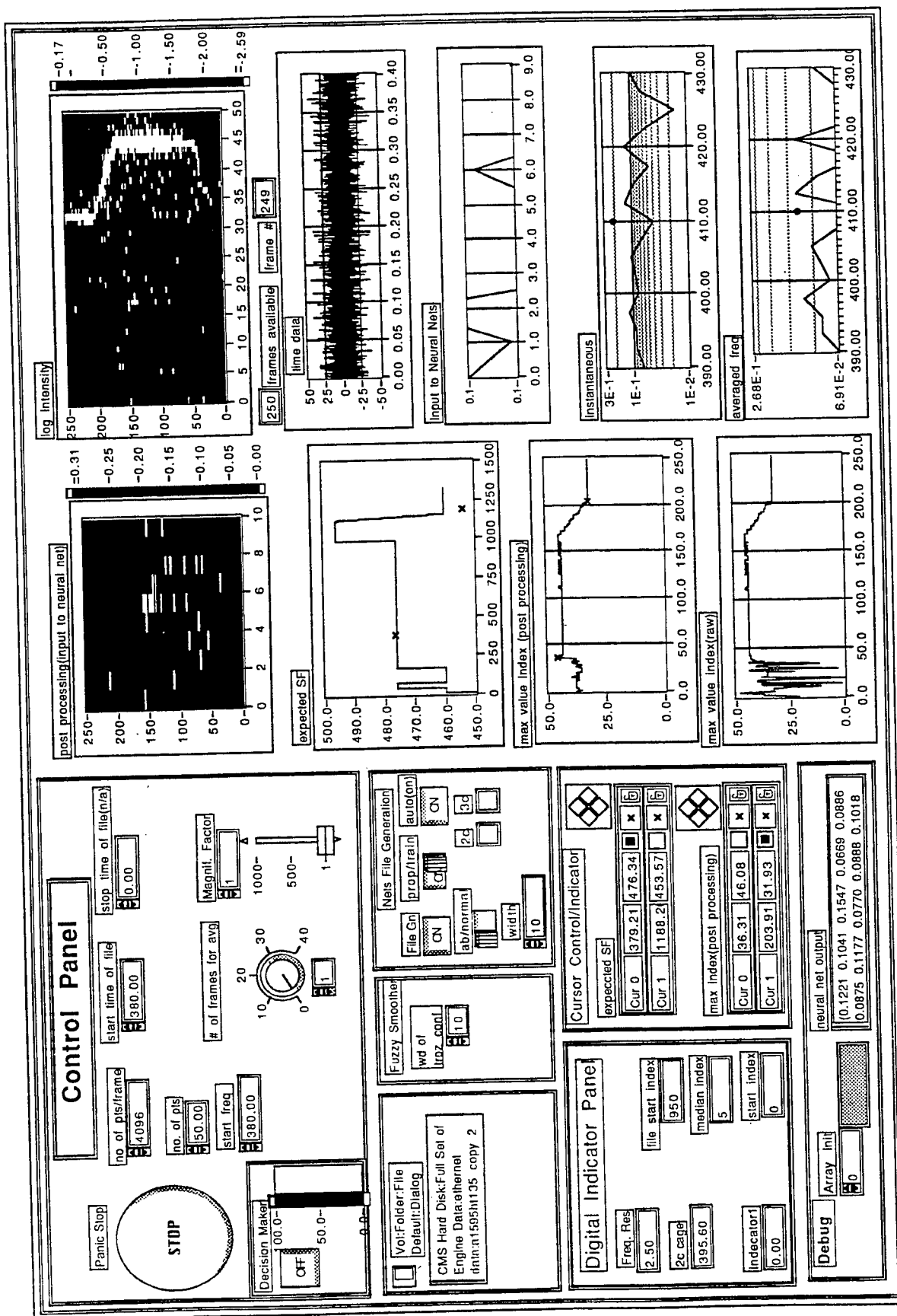
Figure 27. Preprocessor display panel.

REFERENCES

1. Sunnersjo, C.S.: "Rolling Bearing Vibrations—The Effect of Geometrical Imperfections and Wear." Journal of Sound and Vibration, vol. 98(4),1985, pp. 455–474.

2. McFadden, P.D., and Smith, J.D.: "Model for the Vibration Produced by a Single Point Defect in a Rolling Element Bearing." Journal of Sound and Vibration, vol. 96(1), 1984, pp. 69–82.

3. Pearson, E.S., and Hartley, H.O.: "Biometrica Tables for Stasticians." vol. 1, Third Ed., Cambridge.

4. Weaver, H.J.: "Applications of Discrete and Continuous Fourier Analysis." John Wiley and Sons, 1983, pp. 340–346.

BIBLIOGRAPHY

Kandel, E.R., and Hawkins, R.D.: "The Biological Basis of Learning and Individuality." Scientific American, Special Issue: Mind and Brain, 1992, pp. 79–86.

Brainbridge, L.: "The Process Controller." in W.T. Singleton's "The Study of Real Skills." Academic Press, New York, 1976.

Dietz, W.E., Kiech, E.L., and Ali, M.: "Jet and Rocket Engine Fault Diagnosis in Real Time." Journal of Neural Network Computing, vol. 1, No. 1, 1989, pp 5–18.

Duyar, A., and Merrill, W.: "Fault Diagnosis for the Space Shuttle Main Engine." Journal of Guidance, Control, and Dynamics, vol. 15, No. 2, March–April 1992, pp. 384–389.

Hine, M.J.: Absolute Ball Bearing Wear Measurements From SSME Turbopump Dynamic Signals." Journal of Sound and Vibration, vol. 128(2), 1989, pp. 321–331.

Horak, D.T.: "Failure Detection in Dynamics System With Modeling Error." Journal of Guidance, vol. 11, No. 6, pp. 508–571.

Kakagi, T., Sugeno, M.: "Fuzzy Identification of Systems and Its Applications to Modeling and Control." IEEE Transactions on Systems, Man, and Cybernetics (SMC), vol. SMC-15, No. 1, January–February 1985, pp. 116–132.

Kosko, B.: "Neural Networks and Fuzzy Systems." Prentice Hall, 1992.

Merill, W., DeLaat, J., and Bruton, W.: "Advanced Detection, Isolation, and Accommodation of Sensor Failures—Real-Time Evalution." Journal of Guidance, vol. 11, No. 6, November–December 1988, pp. 517–524.

Morrison, J.D.: "A Neural Network Model That Supports Real Time Learning of Temporal Relationships in Complex Engineering Domain." Workshop on Neural Networks 1992, Auburn, AL, 1992.

Negoita, C.V.: "Expert Systems and Fuzzy Systems." The Benjamin/Cummings Publishing Co. Inc., 1985, QA76.9E96 N384 1985.

Sugeno, M., and Kang, G.: "Structure Identification of Fuzzy Model." Fuzzy Set and Systems 28, 1988, pp. 15–33.

Sugeno, M., and Tanaka, K.: "Successive Identification of a Fuzzy Model and Its Application to Prediction of a Complex System." Fuzzy Sets and Systems 42, North-Holland, 1991, pp. 315–334.

Sugeno, M., and Kang. G.: "Fuzzy Modeling and Control of Multilayer Incinerator." Fuzzy Set and System 18, 1986, pp. 326–346.

Tong, R.M.: "A Control Engineering Review of Fuzzy Systems." Automatica, vol. 13, pp. 559–569.

Scientific American, Special Issue, 1992, Mind and Brain.

APPENDIX A

ARTIFICIAL NEURAL NET PARAMETERS

Shift and Propagate Parameters (1 of 2)

W1 =

Columns 1 through 7

-0.2205	0.0255	-0.0294	-0.3790	0.1606	0.2493	-0.2605
1.4083	-1.7710	-0.8315	0.2501	1.6040	0.9984	-0.5730
-0.4572	0.3848	0.4565	0.1258	0.3068	0.1800	0.0555
0.7994	-0.1463	0.1157	1.0177	-1.1560	0.1994	1.6783
-0.8600	-0.6219	-1.2588	-0.5633	-1.2257	-0.1862	-0.8889
-0.4106	0.1560	0.0750	-0.4506	0.1744	-0.2894	-0.1357
0.2012	0.0906	-0.4790	0.0437	-0.9882	0.0499	0.4524
-0.7805	-0.1112	0.0090	-1.3214	0.1259	1.4597	-0.6140
0.5324	-0.3947	0.5893	-0.4454	1.4631	0.6267	1.6365

Columns 8 through 14

-0.0277	-0.3377	-0.5169	0.0042	-0.1252	-0.3800	-0.2069
-1.4170	0.2880	-0.8322	-0.9631	0.6908	0.7943	-0.4423
-0.1385	0.7119	0.0442	-0.2153	0.6068	0.0852	-0.0662
-0.3966	0.2238	1.4413	-0.1822	1.1730	0.7878	-1.3708
-0.9446	0.3958	-0.6383	-0.9919	1.4657	-0.2012	-0.5888
0.0522	0.0559	-0.6805	0.2698	0.0850	-0.1366	0.1491
-1.0306	-0.0861	-0.0553	-0.0379	-0.0984	-0.6341	-0.7628
-0.3548	-0.0027	-0.2003	-1.0442	0.9775	-0.7228	-1.2034
-1.3553	-0.3854	-1.4227	1.7290	0.7316	0.2531	-1.4900

Columns 15 through 21

0.0392	-0.1468	-0.0198	0.2012	-0.4357	0.0108	-0.0449
-1.0089	-0.4127	-0.8799	0.5255	-1.0989	-0.4742	-0.6783
0.2997	0.4256	0.6892	-0.1704	0.8726	-0.0203	0.1180
0.6210	1.0954	-1.9407	0.2896	1.5091	-0.7880	0.5451
1.0726	-0.2837	-1.4759	1.5632	-0.3636	-1.1859	1.5613
-0.2283	-0.2317	0.4223	0.3896	-0.5429	0.0884	0.0201
-0.2043	-0.2694	-0.1676	0.2632	0.3617	-0.5948	-0.0723
-0.0365	-0.5441	-0.4750	-0.4480	-0.6881	-0.4746	-0.7865
-0.8624	-0.2570	1.2159	1.6124	1.0144	0.3667	-0.7992

Columns 22 through 28

-0.2602	-0.1514	-0.0591	-0.5249	-0.1001	-0.0668	-0.3071
-0.7722	-0.4405	-0.4783	0.1422	-0.0324	0.9236	-0.3892
-0.1163	0.4848	0.2305	0.1438	0.2732	0.0927	0.3401
1.2312	-1.1187	0.3375	1.6606	-0.0280	0.9444	2.5016
-0.5115	0.2395	1.4807	-0.1937	0.7012	0.4081	-0.2519
-0.0982	0.1851	0.1720	0.0278	0.1930	0.0812	-0.2950
-0.0676	0.0020	0.4021	-0.0300	-0.5545	-0.5582	0.0947
0.1436	-0.7380	-0.7710	-0.6133	-0.6861	0.9242	-0.5875
0.1552	0.5865	0.4537	0.6174	1.1963	-0.1149	0.8880

Columns 29 through 30

-0.1742	0.2265
-0.6564	-1.1679
1.1624	0.2859
-1.2073	0.5666
0.0228	0.9671
0.3395	0.0209
-1.1591	-0.0423
-0.3808	0.3940
-0.9474	-0.5041

28

Shift and Propagate Parameters (2 of 2)

W2 =

Columns 1 through 7

-1.1118   -3.5790   -2.1850   -2.9365   3.8081   -1.0371   -2.0264

Columns 8 through 9

3.3284   4.1655

B1 =

B2 =

0.5335
-0.4086
0.1243
-0.6208
-0.9886
0.2876
-0.4304
0.2425
1.2105

-0.4554

Rotate and Propagate (13 inputs, 8 hidden neurons, 1 output)

1st Layer Biases:
```
        -6.0074   -4.7994    5.4865    0.0055   -2.2119   -4.2985
         4.9373   -1.3591
```

Hidden Layer Bias:
3.3723

Weights (input-hidden)

Columns 1 through 7

0.4911	2.2876	2.2881	1.9633	-0.8116	-1.5639	1.7701
-0.9976	-1.5030	-1.5826	3.3567	-0.9871	-1.0065	-0.6162
1.8084	-1.8533	-2.4900	1.5960	1.0634	2.7502	-2.5030
3.2808	5.2286	-6.9593	-3.6218	2.2502	1.2916	1.0299
2.6379	1.4729	-0.7750	2.5572	-2.6357	1.3291	-0.0983
-0.4350	2.1847	-2.5339	2.0848	-2.0491	2.3751	-0.2495
0.8536	-4.2720	1.7930	-0.1992	-0.0690	-1.3368	0.0828
1.4957	1.1806	1.3727	-2.3245	1.0137	2.2137	1.3966

Columns 8 through 13

2.5313	2.6961	0.4243	2.9952	-0.1087	-1.0625
-1.8649	3.3189	-0.5528	1.7537	1.2935	1.8594
-2.0789	-1.7765	-0.8283	-0.5580	0.8157	-2.1509
-1.1153	0.9283	2.7956	-0.1261	2.9068	0.0385
-2.6879	-1.9364	0.4412	2.1586	1.8403	1.1141
2.8394	-0.8790	-0.3321	1.6754	-0.7196	2.0685
-0.7195	0.8262	-3.1211	-1.2096	-1.2087	-1.6676
-1.8435	-0.6152	0.8124	-3.2246	-1.9153	-2.5395

Weight (hidden-output)

Columns 1 through 7

2.3926	-2.4301	1.4169	-7.4914	1.3325	-0.5127	-1.6582

Column 8

-0.7188

APPENDIX B

TYPICAL MISSION PROFILE FILE

An Example Thrust Level Schedule
Test 2485

Time (s)	Thrust Level (percent)
0	0
5	100
10	100
10	104
60	104
67	100
80	100

APPENDIX C

RELATED TEST RESULTS
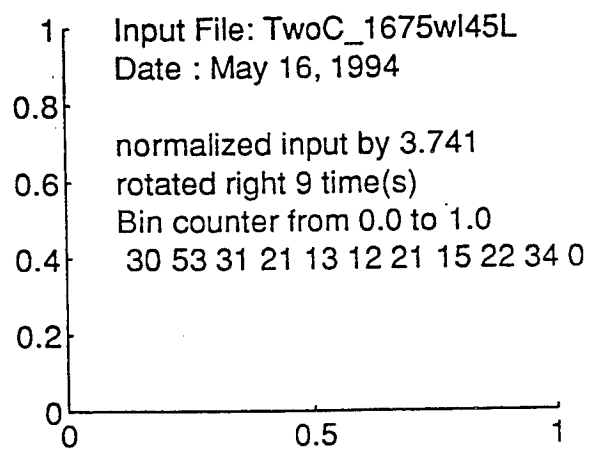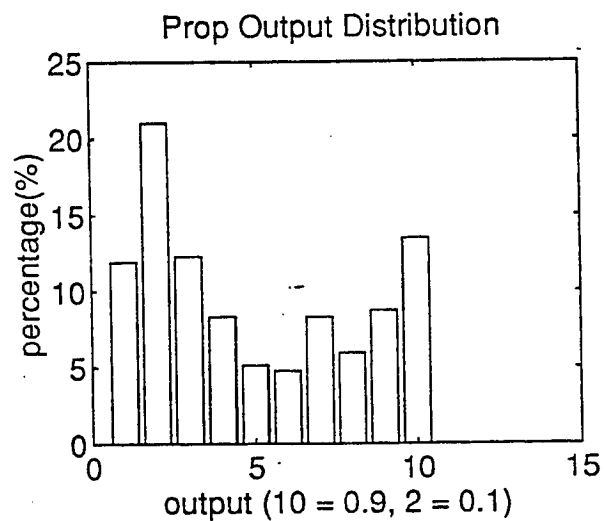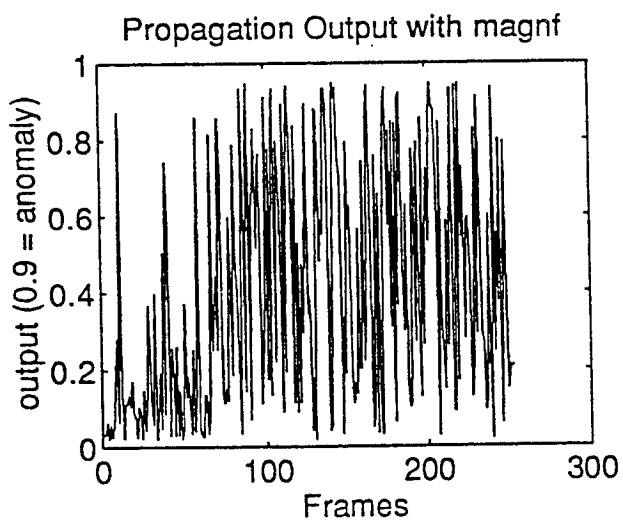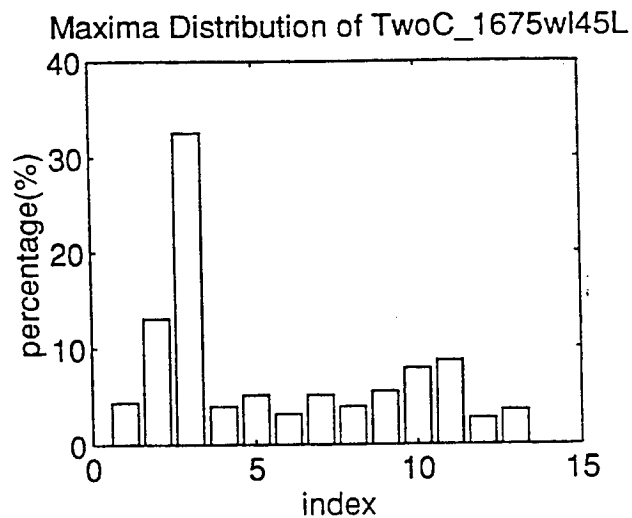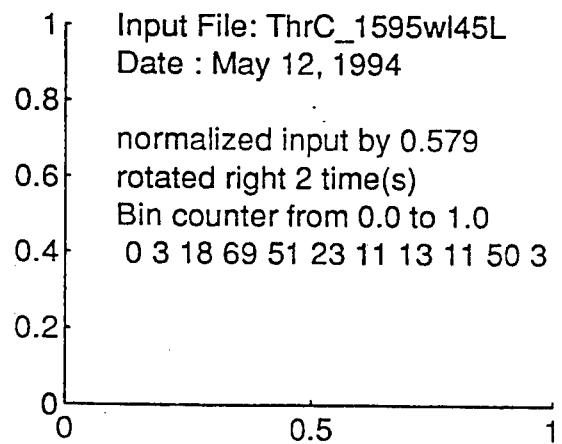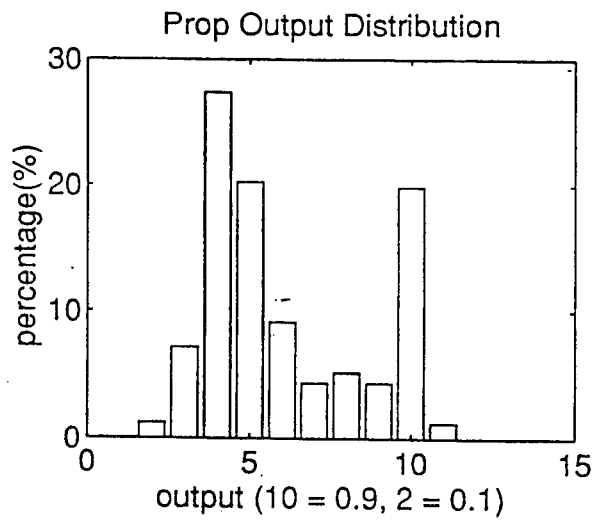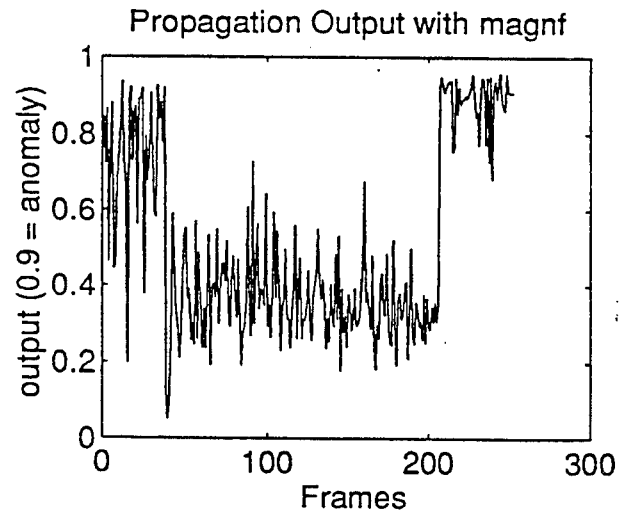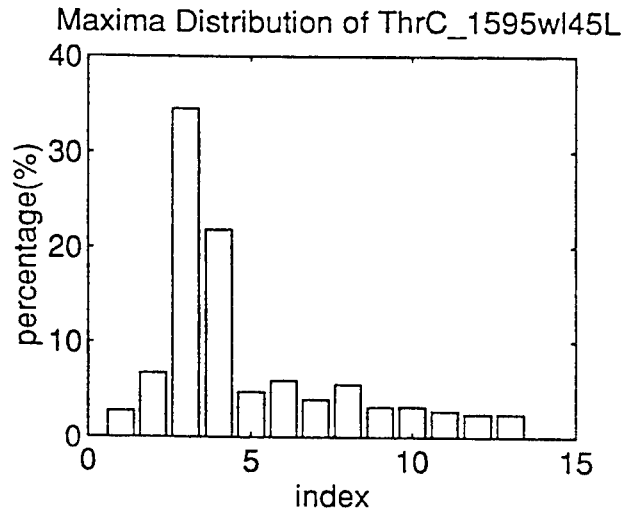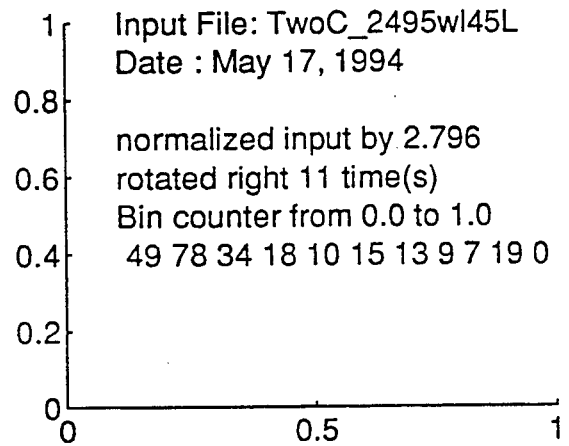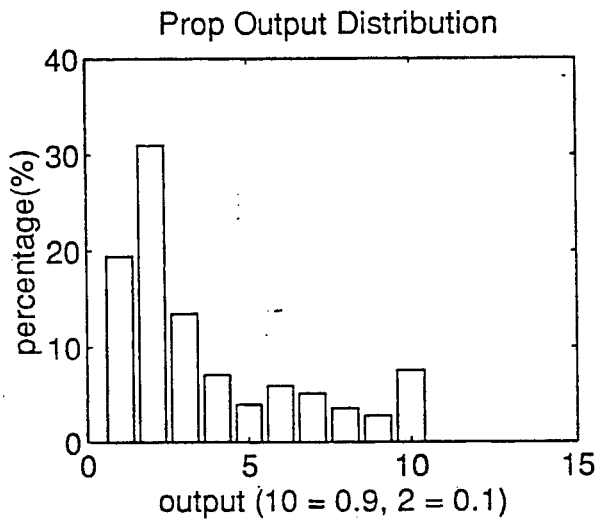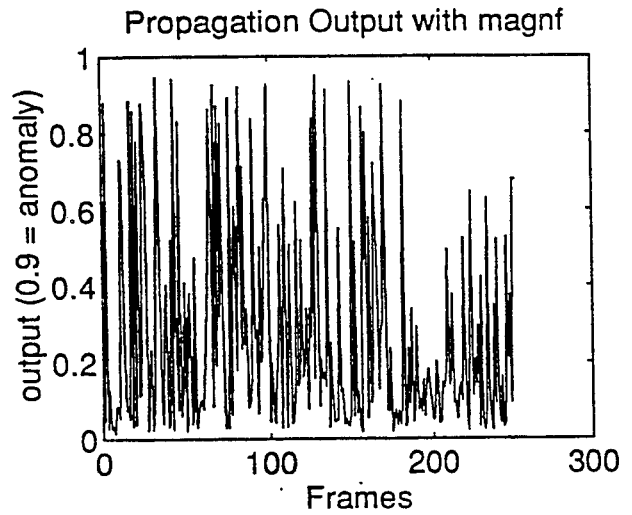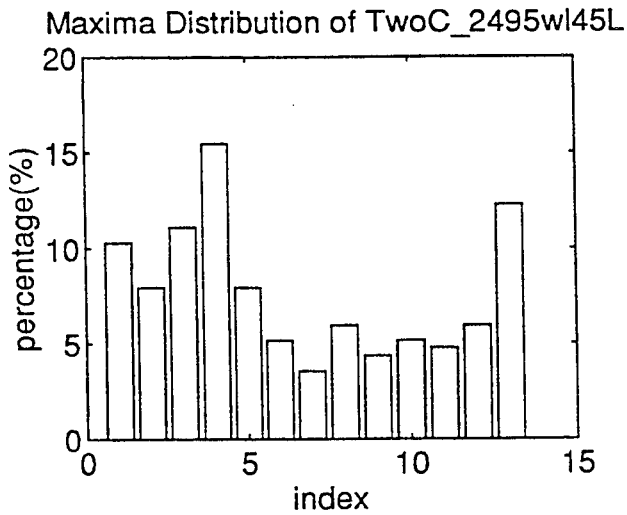
Maxima Distribution of TwoC_1675wl45L

Propagation Output with magnf

Prop Output Distribution

Input File: TwoC_1675wl45L
Date : May 16, 1994

normalized input by 3.741
rotated right 9 time(s)
Bin counter from 0.0 to 1.0
  30 53 31 21 13 12 21 15 22 34 0

Maxima Distribution of ThrC_1595wl45L

Propagation Output with magnf

Prop Output Distribution

Input File: ThrC_1595wl45L
Date : May 12, 1994

normalized input by 0.579
rotated right 2 time(s)
Bin counter from 0.0 to 1.0
 0 3 18 69 51 23 11 13 11 50 3

Maxima Distribution of TwoC_2495wl45L

Propagation Output with magnf

Prop Output Distribution

Input File: TwoC_2495wl45L
Date : May 17, 1994

normalized input by 2.796
rotated right 11 time(s)
Bin counter from 0.0 to 1.0
49 78 34 18 10 15 13 9 7 19 0

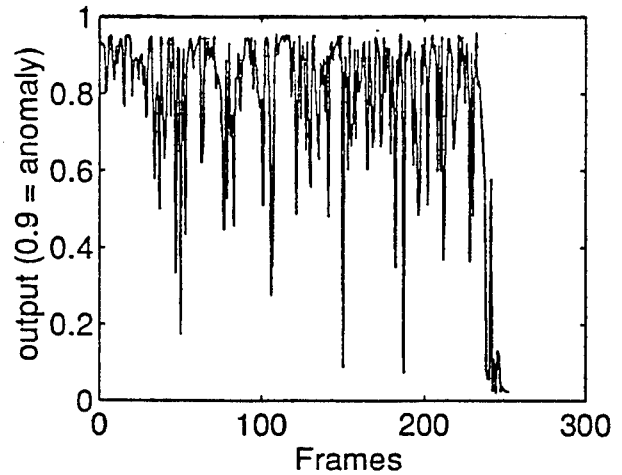## Maxima Distribution of ThrC_446ht13L

Propagation Output with magnf

Prop Output Distribution

Input File: ThrC_446ht13L
Date : May 11, 1994

normalized input by 11.3
rotated right 13 time(s)
Bin counter from 0.0 to 1.0
8 8 1 2 5 11 15 23 42 123 14
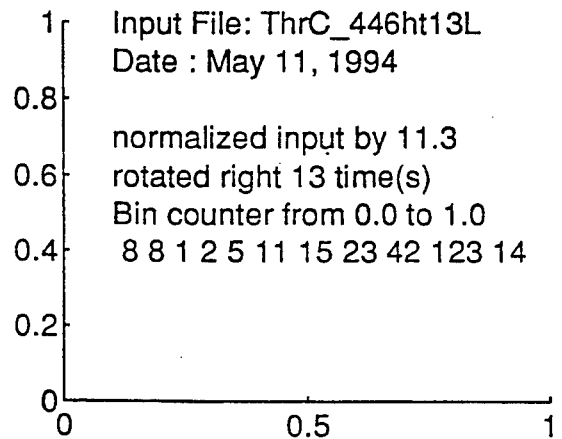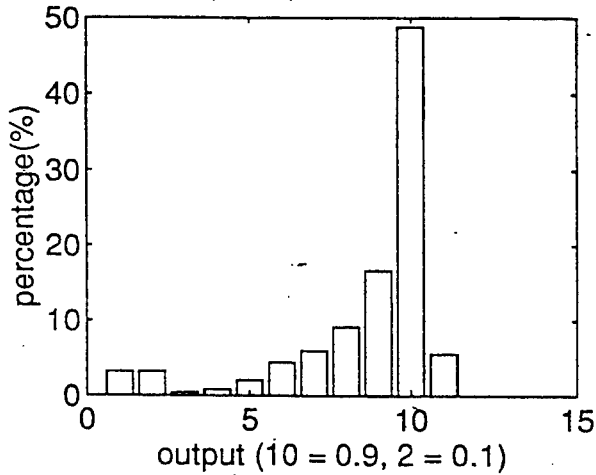
APPROVAL

VEHICLE HEALTH MANAGEMENT USING ADAPTIVE TECHNIQUES— CDDF FINAL REPORT (No. 92-12)

By J.H. Kim and R. Kissel

The information in this report has been reviewed for technical content. Review of any information concerning Department of Defense or nuclear energy activities or programs has been made by the MSFC Security Classification Officer. This report, in its entirety, has been determined to be unclassified.

J.M. McMILLION
Director, Program Development Office

REPORT DOCUMENTATION PAGE

Public reporting burden for this collection of information is estimated to average 1 hour per response, including the time for reviewing instructions, searching existing data sources, gathering and maintaining the data needed, and completing and reviewing the collection of information. Send comments regarding this burden estimate or any other aspect of this collection of information, including suggestions for reducing this burden, to Washington Headquarters Services, Directorate for Information Operations and Reports, 1215 Jefferson Davis Highway, Suite 1204, Arlington, VA 22202-4302, and to the Office of Management and Budget, Paperwork Reduction Project (0704-0188), Washington, DC 20503.

1. AGENCY USE ONLY (Leave blank)	2. REPORT DATE November 1994	3. REPORT TYPE AND DATES COVERED Technical Memorandum

4. TITLE AND SUBTITLE
Vehicle Health Management Using Adaptive Techniques—CDDF
Final Report (No. 92-12)

5. FUNDING NUMBERS

6. AUTHOR(S)
J.H. Kim and R. Kissel

7. PERFORMING ORGANIZATION NAME(S) AND ADDRESS(ES)
George C. Marshall Space Flight Center
Marshall Space Flight Center, Alabama 35812

8. PERFORMING ORGANIZATION REPORT NUMBER

9. SPONSORING/MONITORING AGENCY NAME(S) AND ADDRESS(ES)
National Aeronautics and Space Administration
Washington, DC 20546

10. SPONSORING/MONITORING AGENCY REPORT NUMBER
NASA TM-108472

11. SUPPLEMENTARY NOTES
Prepared by Program Development Office

12a. DISTRIBUTION/AVAILABILITY STATEMENT
Unclassified—Unlimited

12b. DISTRIBUTION CODE

13. ABSTRACT (Maximum 200 words)

Automated engine diagnostics using cognitive computing methodologies is investigated. Space shuttle main engine vibrational data is used to test the algorithms.

14. SUBJECT TERMS
engine diagnostics, cognitive computing, artificial neural nets, fuzzy logic, artificial intelligence, vehicle health management

15. NUMBER OF PAGES
46

16. PRICE CODE
NTIS

17. SECURITY CLASSIFICATION OF REPORT	18. SECURITY CLASSIFICATION OF THIS PAGE	19. SECURITY CLASSIFICATION OF ABSTRACT	20. LIMITATION OF ABSTRACT
Unclassified	Unclassified	Unclassified	Unlimited